Communications in Information and Systems
Volume 23, Number 3, 325–358, 2023

Flow of an incompressible nonlinear bipolar viscous fluid in a sinusoidally constricted channel

Allen Montz, Hamid Bellout, and Frederick Bloom

We seek to analyse blood flow in stenosed vessels within the framework of Non-Newtonian fluids. We analyse the model and seek to highlight the effects of physical parameters on the nature of the flow. Our main goal was to understand the effects of the physical parameters on the qualitative behavior of the flow. We introduce and use approximate solutions as they provide more insight in the qualitative behavior of the flow than blunt numerical resolution for a particular value of the parameters. Some numerical simulations are also provided.

1. Introduction

Steady viscous fluid flow in axisymmetric channels and pipes of varying cross-section has been the subject of numerous studies because it is relevant for a diverse range of problems. An important application of this problem is to blood flow in stenosed vessels. An alteration in the characteristics of blood flow due to stenosis is well known to be associated with the initiation and progression of vascular disease [6]. It is thought that greater knowledge of flow characteristics in the presence of a constriction may help in understanding the complications which arise from stenosis [8]. Flow in wavy channels and pipes also has applications to porous media flow, because it is believed that porous media can be modeled as an array of sinusoidally constricted tubes [7, 10]. We note that, Yoo and Joseph [25], and Ahrens, Yoo, and Joseph [1], studied flow in a wavy channel and pipe, respectively, in order to investigate the change of type in the vorticity.

Previous studies which considered steady flow of a Newtonian fluid in an axisymmetric pipe of varying cross-section, in order to model blood flow in a stenosed vessel, include [6, 8], and [9]. In [6], the authors obtained an asymptotic solution under the assumption of a slowly varying tube wall; with this solution they predicted a critical Reynolds number (inversely proportional to the amplitude of the tube constriction, at which flow separation occurs), axial velocity profiles which exhibit flow reversal near the tube wall, and a

maximum velocity which does not occur along the centerline of the tube for moderate Reynolds numbers. It was found that the shear stress varies in a manner proportional to the amplitude of the wavy wall, with the maximum of the magnitude of the shear stress occurring in the convergent portion of the tube. In [9], the authors performed experiments on the flow of blood in a sinusoidally constricted pipe; they observed that the shear stress varies in a manner proportional to the amplitude of the wavy wall, with the maximum of the magnitude of the shear stress occurring in the convergent portion of the tube. They also found that there exists a critical Reynolds number for which flow separation, and subsequent reattachment, occurs just after the convergent portion of the tube. However, the occurrence of the critical Reynolds numbers for which flow separation occurs is disputed, as noted by Hemmat and Borhan [10], and several numerical studies have predicted flow reversal in the case of Stokes flow.

As the boundary-value problems for steady flow of viscous fluids in axisymmetric channels and pipes of varying cross-section are not amenable to analytic solutions, various methods are available to obtain approximate solutions. A relatively simple method is the lubrication approximation, in which the flow is approximated by assuming Poiseuille flow at each axial location along the channel or tube. Despite the obvious drawbacks, this method provides a good approximation for domains with a mild constriction. More accurate solutions may be obtained if the relevant boundary-value problem is solved numerically, as was done, e.g., in [10] and [7]. A third type of approximate solution, which may be found using a simple analysis and which provides more accurate solutions than the lubrication approximation is the domain perturbation method; it provides asymptotic solutions based upon the assumed smallness of certain parameters of the domain geometry. This technique has been applied, under various assumptions on the domain, for a Newtonian fluid in [6, 20, 23], and [13]. Furthermore, this technique was applied to study the non-Newtonian four constant Oldroyd fluid in [12] and an upper convected Maxwell fluid in [1, 25].

The constitutive theory formulated in [5] for an isothermal, incompressible, nonlinear bipolar viscous fluid assumes the form

$$t_{ij} = -p\delta_{ij} + 2\mu_0(\varepsilon + e_{kl}e_{kl})^{-\alpha/2}e_{ij} - 2\mu_1\Delta e_{ij} \tag{1.1a}$$

$$\tau_{ijk} = 2\mu_1\frac{\partial e_{ij}}{\partial x_k}, \tag{1.1b}$$

where δ_{ij} is the Kronecher delta, t_{ij} and τ_{ijk} are the components of the Cauchy stress tensor and the first multipolar stress tensor, respectively, ε,

μ_0, μ_1, α are constitutive parameters, and the e_{ij} are the components of the rate of deformation tensor

$$e_{ij} = \frac{1}{2}\left(\frac{\partial v_i}{\partial x_j} + \frac{\partial v_j}{\partial x_i}\right), \tag{1.2}$$

the v_i being the components of the velocity vector. It is assumed in [5] that ε, μ_0, μ_1 are positive and that $0 \leq \alpha < 1$; for $\alpha = \mu_1 = 0$, (1.1) reduces to the constitutive relation for a Newtonian fluid as given by the Stokes' law, with the nonlinear viscosity

$$\mu(|\mathbf{e}|) = \mu_0(\varepsilon + e_{kl}e_{kl})^{-\alpha/2} \tag{1.3}$$

reducing to the constant μ_0. We will refer to the *linear bipolar model* as the constitutive theory which results from (1.1) upon formally setting $\alpha = 0$, and the *non-Newtonian model* as the constitutive theory which results from (1.1) upon formally setting $\mu_1 = 0$. The bipolar model (1.1) is a special case of of the broader theory of multipolar viscous fluids, which is consistent with the principle of material frame indifference and the second law of thermodynamics, in the form of the Clausius-Duhem inequality [18]. A comprehensive survey of the theory of incompressible bipolar (and related non-Newtonian) viscous fluids is given in the recent monograph [4].

The recently published paper [17] contains some of the theoretical background and justifications for the approaches and assumptions adopted here.

The study of flow in a wavy, but rigid, domain can be viewed as an initial step in the study of the more general problem of blood flow in a stenosed, elastic vessel. While in medium and large vessels it is well accepted that blood can be modeled as a Newtonian fluid, in small vessels (specifically when the shear rate is less than 100 s^{-1} [6]) blood exhibits behavior typical of a shear-thinning fluid [19]. For results, both theoretical and numerical, on the Newtonian flow of blood in elastic vessels, see [22] and [21], while studies in which blood is assumed non-Newtonian include [15, 24], and [11] (and the references therein).

In this paper we apply the domain perturbation method separately, under two different assumptions on the domain geometry, to study the flow of a bipolar fluid in a sinusoidally constricted channel of small width. First, we follow the work in [1] and [25] by assuming that the dimensionless amplitude of the wall is sufficiently small to justify our asymptotic solution. Next, we follow the work in [6] by assuming the extent of the surface roughness is large when compared with the mean height of the channel.

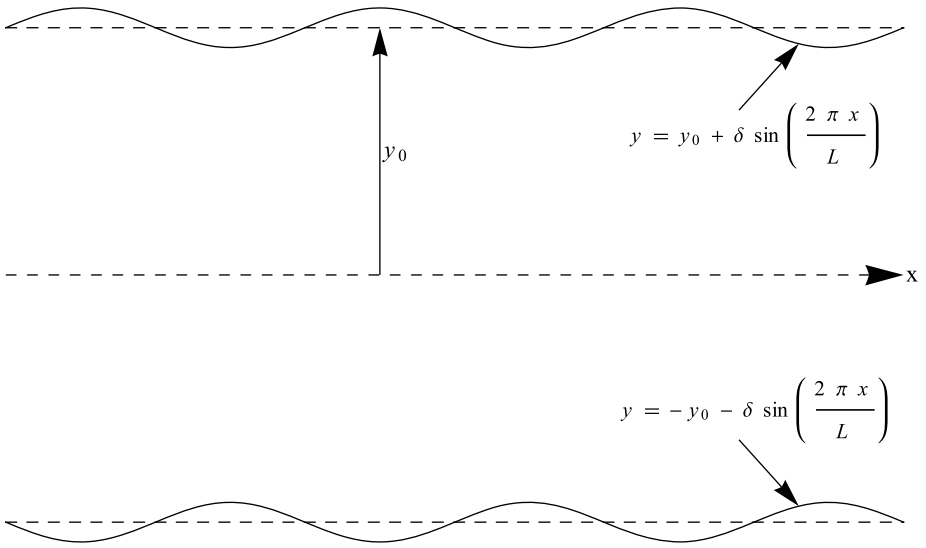

Figure 1: The domain of the problem, Ω_δ.

2. Governing equations

In this paper we restrict ourselves to steady flows in sinusoidally constricted channels (see Figure 1). The domain is given by

$$\Omega_\delta = \{(x, y) \mid -\infty < x < \infty, -y_\delta(x) \le y \le y_\delta(x)\}, \tag{2.1}$$

where $\pm y_\delta(x)$ are the locations of the upper and lower wavy walls, respectively. For the wall boundary we will take

$$y_\delta(x) = y_0 + \delta \sin\left(\frac{2\pi x}{L}\right). \tag{2.2}$$

The height of the unperturbed channel is y_0, the period of the wavy wall is L, and the height of the perturbation is δ.

We will assume a steady velocity field of the form $\mathbf{v} = (u(x, y), v(x, y))$, and a pressure of the form $p = p(x, y)$. Under the assumptions on the steady velocity field, the nonzero components of the rate of deformation tensor, $\mathbf{e}$, are

$$e_{xx} = \frac{\partial u}{\partial x}, \quad e_{xy} = e_{yx} = \frac{1}{2}\left(\frac{\partial u}{\partial y} + \frac{\partial v}{\partial x}\right), \quad e_{yy} = \frac{\partial v}{\partial y}. \tag{2.3}$$

It follows that[1] the boundary-value problem for the flow of an incompressible bipolar viscous fluid, in the domain Ω_δ, is given by

(2.4a)
$$\rho\left(u\frac{\partial u}{\partial x}+v\frac{\partial u}{\partial y}\right)=-\frac{\partial p}{\partial x}+\gamma(|\mathbf{e}|)^{-\alpha/2}\left(\frac{\partial^2 u}{\partial x^2}+\frac{\partial^2 u}{\partial y^2}\right)$$
$$-\frac{\alpha}{2}\gamma(|\mathbf{e}|)^{-\alpha/2-1}\left[\frac{\partial|\mathbf{e}|^2}{\partial x}\frac{\partial u}{\partial x}+\frac{1}{2}\frac{\partial|\mathbf{e}|^2}{\partial y}\left(\frac{\partial u}{\partial y}+\frac{\partial v}{\partial x}\right)\right]$$
$$-\mu_1\left(\frac{\partial^4 u}{\partial x^4}+2\frac{\partial^4 u}{\partial x^2\partial y^2}+\frac{\partial^4 u}{\partial y^4}\right),\quad \text{in } \Omega_\delta,$$

(2.4b)
$$\rho\left(u\frac{\partial v}{\partial x}+v\frac{\partial v}{\partial y}\right)=-\frac{\partial p}{\partial y}+\gamma(|\mathbf{e}|)^{-\alpha/2}\left(\frac{\partial^2 v}{\partial x^2}+\frac{\partial^2 v}{\partial y^2}\right)$$
$$-\frac{\alpha}{2}\gamma(|\mathbf{e}|)^{-\alpha/2-1}\left[\frac{1}{2}\frac{\partial|\mathbf{e}|^2}{\partial x}\left(\frac{\partial u}{\partial y}+\frac{\partial v}{\partial x}\right)+\frac{\partial|\mathbf{e}|^2}{\partial y}\frac{\partial v}{\partial y}\right]$$
$$-\mu_1\left(\frac{\partial^4 v}{\partial x^4}+2\frac{\partial^4 v}{\partial x^2\partial y^2}+\frac{\partial^4 v}{\partial y^4}\right),\quad \text{in } \Omega_\delta,$$

(2.4c)
$$\frac{\partial u}{\partial x}+\frac{\partial v}{\partial y}=0,\quad \text{in } \Omega_\delta,$$

(2.4d)
$$u=v=0,\ \text{at } y=\pm y_\delta(x),$$

(2.4e)
$$2y_\delta'^2\frac{\partial^2 u}{\partial x^2}-y_\delta'(1-y_\delta'^2)\frac{\partial^2 v}{\partial x^2}-y_\delta'(3-y_\delta'^2)\frac{\partial^2 u}{\partial x\partial y}+(1-3y_\delta'^2)\frac{\partial^2 v}{\partial x\partial y}$$
$$+(1-y_\delta'^2)\frac{\partial^2 u}{\partial y^2}+2y_\delta'^2\frac{\partial^2 v}{\partial y^2}=0,\quad \text{at } y=y_\delta(x),$$

and

(2.4f)
$$2y_\delta'^2\frac{\partial^2 u}{\partial x^2}+y_\delta'(1-y_\delta'^2)\frac{\partial^2 v}{\partial x^2}+y_\delta'(3-y_\delta'^2)\frac{\partial^2 u}{\partial x\partial y}+(1-3y_\delta'^2)\frac{\partial^2 v}{\partial x\partial y}$$
$$+(1-y_\delta'^2)\frac{\partial^2 u}{\partial y^2}+2y_\delta'^2\frac{\partial^2 v}{\partial y^2}=0,\quad \text{at } y=-y_\delta(x).$$

[1]A full derivation of the boundary-value problem for an incompressible bipolar viscous fluid in a channel with the upper and lower walls given by a function symmetric about the centerline of the channel is given in Appendix B of the thesis [16].

In (2.4), ρ is the constant mass density and $\gamma(|\mathbf{e}|) = \mu_0(\varepsilon + |\mathbf{e}|^2)$. The higher order boundary conditions (2.4e) and (2.4f) are required due to the dependence of the bipolar model on third order spatial gradients of the velocity. These boundary conditions are a rigorous consequence of the principal of virtual work; it is shown in [3] that the general higher order boundary conditions for the initial-boundary value problem for bipolar viscous fluid flows in a domain Ω with smooth boundary $\partial\Omega$ are given by

$$\tau_{ijk}\nu_j\nu_k - \tau_{ljk}\nu_l\nu_j\nu_k\nu_i = 0, \quad i = 1,2,3 \quad \text{on } \partial\Omega. \tag{2.5}$$

In (2.5), the ν_i are the components of the exterior unit normal of $\partial\Omega$ and it is understood that we sum on repeated indices. The boundary conditions (2.4e) and (2.4f) follow from (2.5), upon applying the definition of τ_{ijk} as given in (1.1b), the assumptions on the velocity field, the assumed form of the domain, and the fact that the exterior unit normal of Ω_δ is given by

$$\boldsymbol{\nu} = \frac{(-y_\delta'(x), 1, 0)}{\sqrt{1 + (y_\delta'(x))^2}}. \tag{2.6}$$

The boundary-value problem for the linear bipolar fluid follows from (2.4) upon setting $\alpha = 0$, while the boundary-value problem for the non-Newtonian fluid follows from (2.4) upon setting $\mu_1 = 0$ and dropping the higher order boundary conditions (2.4e) and (2.4f). Finally, the boundary-value problem for the Newtonian fluid follows from the non-Newtonian boundary-value problem upon setting $\alpha = 0$.

With $\delta = 0$, the domain is the channel with flat walls given by $\Omega_0 = \{(x, y) \mid -\infty < x < \infty, -y_0 \le y \le y_0\}$; in this case we assume Poiseuille flow and seek a solution to (2.4), as well as its reductions to the case of the linear bipolar, non-Newtonian, and Newtonian fluid, of the form $\mathbf{v} = (u(y; \alpha, \varepsilon, \mu_1), 0)$, where we have explicitly denoted the dependence of u on the constitutive parameters. For the linear bipolar fluid the boundary-value problem in the domain Ω_0 is given by

$$\mu_0 u'' - \mu_1 u'''' = -G, \quad \text{in } \Omega_0, \tag{2.7a}$$

$$u(\pm y_0) = 0 \quad \text{and} \quad u''(\pm y_0) = 0, \tag{2.7b}$$

where, G is the constant pressure gradient. The solution of (2.7) is given by

$$u(y; 0, 0, \mu_1) = \frac{G}{2\mu_0^2}\left[\mu_0\left(y_0^2 - y^2\right) - 2\mu_1\left(1 - \operatorname{sech}\left(\sqrt{\frac{\mu_0}{\mu_1}}y_0\right)\cosh\left(\sqrt{\frac{\mu_0}{\mu_1}}y\right)\right)\right]. \tag{2.8}$$

If we set $\mu_1 = 0$ in (2.8) we obtain the classical solution for Poiseuille flow of a Newtonian fluid in the channel, i.e.,

$$u(y;0,0,0) = \frac{G}{2\mu_0}(y_0^2 - y^2). \tag{2.9}$$

Note that, as $\mu_1 \to 0^+$, $u_0(y;0,0,\mu_1) \to u_0(y;0,0,0)$, since we have, for $y \in [-y_0, y_0]$,

$$0 \leq \left| \mu_1 \operatorname{sech}\left(\sqrt{\frac{\mu_0}{\mu_1}} y_0\right) \cosh\left(\sqrt{\frac{\mu_0}{\mu_1}} y\right) \right| = |\mu_1|. \tag{2.10}$$

As μ_1 increases from zero, the profiles of (2.8) deviate from the classical parabolic profiles and begin to flatten out.

For a nonlinear bipolar or non-Newtonian fluid it is not possible to find a closed form Poiseuille flow solution; however, it has been demonstrated in [5] that there exists a unique solution $u(y;\alpha,\varepsilon,\mu_1)$ of the bipolar Poiseuille flow boundary-value problem, which depends continuously on the parameters α, ε, and μ_1. Specifically, it was proven in [5] that $u(y;\alpha,\varepsilon,\mu_1) \to u(y;\alpha,\varepsilon,0)$, as $\mu_1 \to 0^+$, in $C^{1+\sigma}$ for $0 < \sigma < \frac{1}{2}$. Furthermore, the continuous dependence of $u(y;\alpha,\varepsilon,\mu_1)$ on ε and μ_1 was made explicit in [2].

We will proceed by working with dimensionless variables. Employing a standard approach (e.g., see [14] for a similar nondimensionalization), we set

$$\bar{x} = \frac{x}{L}, \quad \bar{y} = \frac{y}{y_0}, \quad \bar{u} = \frac{u}{U}, \quad \bar{v} = \frac{v}{V}, \quad \bar{p} = \frac{p}{P}. \tag{2.11}$$

For $\alpha \neq 0$, the parameter μ_0 does not have the units of viscosity; this is due to the term $(\varepsilon + |\mathbf{e}|^2)^{-\alpha/2}$ which is present in the nonlinear viscosity, $\mu(|\mathbf{e}|)$, and which has units of $time^{\alpha}$. Therefore, for $\alpha \neq 0$, the constant μ_0 has units of $mass \times (distance \times time^{1+\alpha})^{-1}$, while for $\alpha = 0$, μ_0 has the units of viscosity. To nondimensionalize the nonlinear viscosity, we write it in terms of a parameter, $\mu_0^{NS} := \mu_0 \varepsilon^{-\alpha/2}$, which has the units of viscosity, times a dimensionless quantity:

$$\begin{aligned} \mu(|\mathbf{e}|) &= \mu_0(\varepsilon + |\mathbf{e}|^2)^{-\alpha/2} \\ &= \mu_0^{NS}(1 + \varepsilon^{-1}|\mathbf{e}|^2)^{-\alpha/2}, \end{aligned} \tag{2.12}$$

We thus have that

$$\mu_0 = \mu_0^{NS}\varepsilon^{\alpha/2} \to \mu_0^{NS}, \text{ as } \alpha \to 0^+. \tag{2.13}$$

We take $U = \frac{Gy_0^2}{\mu_0^{NS}}$; when $\alpha = 0$, U reduces to the solution (2.9) of the Navier-Stokes equations with $\delta = 0$ along the center-line of the channel. The natural choices for the characteristic velocity in the vertical direction, $V = \frac{y_0 U}{L}$, and the characteristic pressure, $P = GL$, are made clear upon substituting the dimensionless variables (2.11) into the boundary-value problem (2.4). As δ has the units of length, we also introduce a dimensionless wall amplitude

$$\bar{\delta} = \frac{\delta}{y_0}. \tag{2.14}$$

It now follows that the nondimensional wall boundary is given by $\bar{y}_{\bar{\delta}}(\bar{x}) = 1 + \bar{\delta}\sin(2\pi\bar{x})$.

In order to seek a solution to (2.4) in the form of a perturbation expansion, we linearize the nonlinear viscosity, $\mu(|\mathbf{e}|)$, by calculating the rate of deformation tensor $\mathbf{e}$ using a given velocity u_0. We take u_0 to be the solution in a flat wall channel for the linear bipolar fluid, as given by (2.8). The only nonzero components of $\mathbf{e}(u_0)$ in this case are $e_{xy} = e_{yx} = \frac{1}{2}u_0'(y)$, and it follows that $|\mathbf{e}(u_0)|^2 = \frac{1}{2}u_0'^2$.

Applying the transformation (2.11) to the boundary-value problem (2.4), together with the above linearization of the nonliner viscosity, a straightforward calculation yields the following dimensionless form of the boundary-value problem (2.4):

(2.15a)
$$\begin{aligned} R_e\lambda\left(\bar{u}\frac{\partial\bar{u}}{\partial\bar{x}} + \bar{v}\frac{\partial\bar{u}}{\partial\bar{y}}\right) &= -\frac{\partial\bar{p}}{\partial\bar{x}} + F_1\left(\lambda^2\frac{\partial^2\bar{u}}{\partial\bar{x}^2} + \frac{\partial^2\bar{u}}{\partial\bar{y}^2}\right) \\ &\quad + \frac{1}{2}F_1'\left(\frac{\partial\bar{u}}{\partial\bar{y}} + \lambda^2\frac{\partial\bar{v}}{\partial\bar{x}}\right) \\ &\quad - \beta\left(\lambda^4\frac{\partial^4\bar{u}}{\partial\bar{x}^4} + 2\lambda^2\frac{\partial^4\bar{u}}{\partial\bar{x}^2\partial\bar{y}^2} + \frac{\partial^4\bar{u}}{\partial\bar{y}^4}\right), \quad \text{in } \Omega_\delta, \end{aligned}$$

(2.15b)
$$\begin{aligned} R_e\lambda\left(\bar{u}\frac{\partial\bar{v}}{\partial\bar{x}} + \bar{v}\frac{\partial\bar{v}}{\partial\bar{y}}\right) &= -\frac{1}{\lambda^2}\frac{\partial\bar{p}}{\partial\bar{y}} + F_1\left(\lambda^2\frac{\partial^2\bar{v}}{\partial\bar{x}^2} + \frac{\partial^2\bar{v}}{\partial\bar{y}^2}\right) \\ &\quad + F_1'\frac{\partial\bar{v}}{\partial\bar{y}} - \beta\left(\lambda^4\frac{\partial^4\bar{v}}{\partial\bar{x}^4} + 2\lambda^2\frac{\partial^4\bar{v}}{\partial\bar{x}^2\partial\bar{y}^2} + \frac{\partial^4\bar{v}}{\partial\bar{y}^4}\right), \quad \text{in } \Omega_\delta, \end{aligned}$$

$$\frac{\partial\bar{u}}{\partial\bar{x}} + \frac{\partial\bar{v}}{\partial\bar{y}} = 0, \text{ in } \Omega_\delta, \tag{2.15c}$$

$$\bar{u} = \bar{v} = 0, \text{ at } \bar{y} = \pm\bar{y}_{\bar{\delta}}(\bar{x}), \tag{2.15d}$$

(2.15e)

$$2\lambda^4\bar{y}_{\bar{\delta}}'^2\frac{\partial^2\bar{u}}{\partial\bar{x}^2}-\lambda^4\bar{y}_{\bar{\delta}}'(1-\lambda^2y_{\delta}'^2)\frac{\partial^2\bar{v}}{\partial\bar{x}^2}-\lambda^2\bar{y}_{\bar{\delta}}'(3-\lambda^2\bar{y}_{\bar{\delta}}'^2)\frac{\partial^2\bar{u}}{\partial\bar{x}\partial\bar{y}}$$
$$+\lambda^2(1-3\lambda^2\bar{y}_{\bar{\delta}}'^2)\frac{\partial^2\bar{v}}{\partial\bar{x}\partial\bar{y}}+(1-\lambda^2\bar{y}_{\bar{\delta}}'^2)\frac{\partial^2\bar{u}}{\partial\bar{y}^2}+2\lambda^3\bar{y}_{\bar{\delta}}'^2\frac{\partial^2\bar{v}}{\partial\bar{y}^2}=0,\ \text{at}\ \bar{y}=\bar{y}_{\bar{\delta}}(\bar{x}),$$

(2.15f)

$$2\lambda^4\bar{y}_{\bar{\delta}}'^2\frac{\partial^2\bar{u}}{\partial\bar{x}^2}+\lambda^4\bar{y}_{\bar{\delta}}'(1-\lambda^2y_{\delta}'^2)\frac{\partial^2\bar{v}}{\partial\bar{x}^2}+\lambda^2\bar{y}_{\bar{\delta}}'(3-\lambda^2\bar{y}_{\bar{\delta}}'^2)\frac{\partial^2\bar{u}}{\partial\bar{x}\partial\bar{y}}$$
$$+\lambda^2(1-3\lambda^2\bar{y}_{\bar{\delta}}'^2)\frac{\partial^2\bar{v}}{\partial\bar{x}\partial\bar{y}}+(1-\lambda^2\bar{y}_{\bar{\delta}}'^2)\frac{\partial^2\bar{u}}{\partial\bar{y}^2}+2\lambda^3\bar{y}_{\bar{\delta}}'^2\frac{\partial^2\bar{v}}{\partial\bar{y}^2}=0,\ \text{at}\ \bar{y}=-\bar{y}_{\bar{\delta}}(\bar{x}).$$

In (2.15), we have defined the Reynolds number to be

$$R_e=\frac{\rho y_0U}{\mu_0^{NS}},\tag{2.16}$$

the dimensionless parameters λ and β by

$$\lambda=\frac{y_0}{L}\quad\text{and}\quad\beta=\frac{\mu_1}{\mu_0y_0^2},\tag{2.17}$$

and, for ease of notation, set

$$F_1(\bar{y})=\left(1+\frac{1}{2}\varepsilon^{-1}\left(\frac{U}{y_0}\right)^2\bar{u}_0'^2\right)^{-\alpha/2}.\tag{2.18}$$

The dimensionless form of the boundary-value problem for linear bipolar fluid follows from (2.15) upon setting $\alpha=0$. The dimensionless form of the non-Newtonian boundary-value problem follows from (2.15) upon setting $\beta=0$ and dropping the higher order boundary conditions (2.15e) and (2.15f); furthermore, if in addition $\alpha=0$, the dimensionless form of the boundary-value problem for the Newtonian fluid is obtained.

3. Perturbation expansion in $\bar{\delta}$

We seek a solution to (2.15) in the form of a regular perturbation expansion in $\bar{\delta}$ of the form

$$\bar{u}(\bar{x},\bar{y})=\bar{u}_0(\bar{y})+\bar{\delta}\bar{u}_1(\bar{x},\bar{y})+O(\bar{\delta}^2),\tag{3.1a}$$

$$\bar{v}(\bar{x},\bar{y}) = \bar{\delta}\bar{v}_1(\bar{x},\bar{y}) + O(\bar{\delta}^2), \tag{3.1b}$$

$$\bar{p}(\bar{x},\bar{y}) = -\bar{x} + \bar{\delta}\bar{p}_1(\bar{x},\bar{y}) + O(\bar{\delta}^2). \tag{3.1c}$$

In (3.1), the zeroth order solution is the Poiseuille flow solution for the linear bipolar fluid. Recalling the solution (2.8), we have, upon applying the transformation (2.11), that

$$\bar{u}_0(\bar{y}) = \frac{1}{2}(1-\bar{y}^2) - \beta\left(1 - \operatorname{sech}\left(\frac{1}{\sqrt{\beta}}\right)\cosh\left(\frac{\bar{y}}{\sqrt{\beta}}\right)\right). \tag{3.2}$$

To find a solution to (2.15), of the form (3.1), we apply the domain perturbation method [14], the key to which is to derive an asymptotically equivalent form of the the boundary conditions (2.15d), (2.15e), and (2.15f). As in [14] or [1], we first take a Taylor expansion in $\bar{\delta}$ to approximate $\bar{u}$ at $\bar{y} = \bar{y}_{\bar{\delta}}(\bar{x})$ in terms of $\bar{u}$ and its derivatives evaluated at $\bar{y} = 1$. Thus, to first order in $\bar{\delta}$, the boundary condition (2.15d) is

$$\begin{aligned} 0 = \bar{u}(\bar{x},\bar{y}_{\bar{\delta}}(\bar{x})) &= \bar{u}(\bar{x},1) + \bar{\delta}\frac{\partial\bar{u}}{\partial\bar{y}}\bigg|_{\bar{y}=1}\frac{\partial\bar{y}_{\bar{\delta}}}{\partial\bar{\delta}}\bigg|_{\bar{\delta}=0} \\ &= \bar{u}(\bar{x},1) + \bar{\delta}\sin(2\pi\bar{x})\frac{\partial\bar{u}}{\partial\bar{y}}\bigg|_{\bar{y}=1}. \end{aligned} \tag{3.3}$$

Inserting the perturbation expansions in (3.1) into (3.3) yields

$$\begin{aligned} 0 &= \left[\bar{u}_0(1) + \bar{\delta}\bar{u}_1(\bar{x},1)\right] + \bar{\delta}\sin(2\pi\bar{x})\left[\bar{u}_0'(1) + \bar{\delta}\frac{\partial\bar{u}_1}{\partial\bar{y}}\bigg|_{\bar{y}=1}\right] \\ &= \bar{u}_0(1) + \bar{\delta}\left[\bar{u}_1(\bar{x},1) + \sin(2\pi\bar{x})\bar{u}_0'(1)\right] + O(\bar{\delta}^2). \end{aligned} \tag{3.4}$$

It follows from (3.4) that the $O(\bar{\delta})$ asymptotically equivalent form of the boundary condition (2.15d), at $\bar{y} = \bar{y}_{\bar{\delta}}(\bar{x})$, is

$$\bar{u}_1(\bar{x},1) = -\sin(2\pi\bar{x})\bar{u}_0'(1). \tag{3.5}$$

A similar calculation for $\bar{v}$ shows that

$$\bar{v}_1(\bar{x},1) = 0. \tag{3.6}$$

Similarly, for the boundary $\bar{y} = -\bar{y}_{\bar{\delta}}(\bar{x})$, we find that

$$\bar{u}_1(\bar{x},-1) = \sin(2\pi\bar{x})\bar{u}_0'(-1) \tag{3.7}$$

and

$$\bar{v}_1(\bar{x}, -1) = 0. \tag{3.8}$$

We now derive asymptotically equivalent forms of the higher order boundary conditions (2.15e) and (2.15f). Recalling that $\bar{y}_{\bar{\delta}} = O(\bar{\delta})$, (2.15e) and (2.15f), to first order in $\bar{\delta}$, are

$$-\lambda^4 \bar{y}'_{\bar{\delta}} \frac{\partial^2 \bar{v}}{\partial \bar{x}^2} - 3\lambda^2 \bar{y}'_{\bar{\delta}} \frac{\partial^2 \bar{u}}{\partial \bar{x} \partial \bar{y}} + \lambda^2 \frac{\partial^2 \bar{v}}{\partial \bar{x} \partial \bar{y}} + \frac{\partial^2 \bar{u}}{\partial \bar{y}^2} = 0, \text{ at } \bar{y} = \bar{y}_{\bar{\delta}}(\bar{x}) \tag{3.9}$$

and

$$\lambda^4 \bar{y}'_{\bar{\delta}} \frac{\partial^2 \bar{v}}{\partial \bar{x}^2} + 3\lambda^2 \bar{y}'_{\bar{\delta}} \frac{\partial^2 \bar{u}}{\partial \bar{x} \partial \bar{y}} + \lambda^2 \frac{\partial^2 \bar{v}}{\partial \bar{x} \partial \bar{y}} + \frac{\partial^2 \bar{u}}{\partial \bar{y}^2} = 0, \text{ at } \bar{y} = -\bar{y}_{\bar{\delta}}(\bar{x}) \tag{3.10}$$

respectively. Substituting the expansions (3.1) into (3.9), we find that, to first order in $\bar{\delta}$,

$$\lambda^2 \bar{\delta} \frac{\partial^2 \bar{v}_1}{\partial \bar{x} \partial \bar{y}} + \bar{u}_0'' + \bar{\delta} \frac{\partial^2 \bar{u}_1}{\partial \bar{y}^2} = 0, \text{ at } \bar{y} = \bar{y}_{\bar{\delta}}(\bar{x}). \tag{3.11}$$

Therefore, the first order in $\bar{\delta}$ higher order boundary condition is

$$\lambda^2 \frac{\partial^2 \bar{v}_1}{\partial \bar{x} \partial \bar{y}} + \frac{\partial^2 \bar{u}_1}{\partial \bar{y}^2} = 0, \text{ at } \bar{y} = \bar{y}_{\bar{\delta}}(\bar{x}). \tag{3.12}$$

A similar calculation for (3.10) yields

$$\lambda^2 \frac{\partial^2 \bar{v}_1}{\partial \bar{x} \partial \bar{y}} + \frac{\partial^2 \bar{u}_1}{\partial \bar{y}^2} = 0, \text{ at } \bar{y} = -\bar{y}_{\bar{\delta}}(\bar{x}). \tag{3.13}$$

If we now expand the terms $\frac{\partial^2 \bar{u}_1}{\partial \bar{y}^2}$ and $\frac{\partial^2 \bar{v}_1}{\partial \bar{x} \partial \bar{y}}$ in Taylor series about $\bar{\delta} = 0$, substitute these expansions into (3.12) and (3.13), and factor out $\bar{\delta}$, it follows immediately that the first order in $\bar{\delta}$ asymptotically equivalent form of the higher order boundary conditions are

$$\lambda^2 \frac{\partial^2 \bar{v}_1}{\partial \bar{x} \partial \bar{y}} + \frac{\partial^2 \bar{u}_1}{\partial \bar{y}^2} = 0, \text{ at } \bar{y} = \pm 1. \tag{3.14}$$

Finally, combining the equations which result from (2.15a), (2.15b), and (2.15c) and the perturbation expansion (3.1), along with the boundary conditions (3.5), (3.6), (3.7), and (3.8), and the higher order boundary

conditions (3.14), the complete boundary-value problem (2.15), to first order in $\bar{\delta}$, is

(3.15a)
$$R_e\lambda\left(\bar{u}_0\frac{\partial\bar{u}_1}{\partial\bar{x}}+\bar{u}_0'\bar{v}_1\right)=-\frac{\partial\bar{p}_1}{\partial\bar{x}}+F_1\left(\lambda^2\frac{\partial^2\bar{u}_1}{\partial\bar{x}^2}+\frac{\partial^2\bar{u}_1}{\partial\bar{y}^2}\right)+\frac{1}{2}F_1'\left(\frac{\partial\bar{u}_1}{\partial\bar{y}}+\lambda^2\frac{\partial\bar{v}_1}{\partial\bar{x}}\right)-\beta\left(\lambda^4\frac{\partial^4\bar{u}_1}{\partial\bar{x}^4}+2\lambda^2\frac{\partial^4\bar{u}_1}{\partial\bar{x}^2\partial\bar{y}^2}+\frac{\partial^4\bar{u}_1}{\partial\bar{y}^4}\right),$$

(3.15b)
$$R_e\lambda\bar{u}_0\frac{\partial\bar{v}_1}{\partial\bar{x}}=-\frac{1}{\lambda^2}\frac{\partial\bar{p}_1}{\partial\bar{y}}+F_1\left(\lambda^2\frac{\partial^2\bar{v}_1}{\partial\bar{x}^2}+\frac{\partial^2\bar{v}_1}{\partial\bar{y}^2}\right)+F_1'\frac{\partial\bar{v}_1}{\partial\bar{y}}-\beta\left(\lambda^4\frac{\partial^4\bar{v}_1}{\partial\bar{x}^4}+2\lambda^2\frac{\partial^4\bar{v}_1}{\partial\bar{x}^2\partial\bar{y}^2}+\frac{\partial^4\bar{v}_1}{\partial\bar{y}^4}\right),$$

(3.15c)
$$\frac{\partial\bar{u}_1}{\partial\bar{x}}+\frac{\partial\bar{v}_1}{\partial\bar{y}}=0,$$

(3.15d)
$$\bar{u}_1(\bar{x},\pm1)=\mp\bar{u}_0'(\pm1)\sin(2\pi\bar{x}),$$

(3.15e)
$$\bar{v}_1(\bar{x},\pm1)=0,$$

(3.15f)
$$\lambda^2\frac{\partial^2\bar{v}_1}{\partial\bar{x}\partial\bar{y}}+\frac{\partial^2\bar{u}_1}{\partial\bar{y}^2}=0,\ \text{at}\ \bar{y}=\pm1.$$

We now introduce the $O(\bar{\delta})$ streamfunction $\bar{\psi}_1(\bar{x},\bar{y})$, defined by

(3.16)
$$\bar{u}_1=\frac{\partial\bar{\psi}_1}{\partial\bar{y}}\quad\text{and}\quad\bar{v}_1=-\frac{\partial\bar{\psi}_1}{\partial\bar{x}}.$$

Differentiating (3.15a) with respect to $\bar{y}$ and adding (3.15b), after differentiating it with respect to $\bar{x}$ and multiplying by $-\lambda^2$, yields, in conjunction with (3.16), the equation

(3.17)
$$R_e\lambda\left(\bar{u}_0\frac{\partial^3\bar{\psi}_1}{\partial\bar{y}^2\partial\bar{x}}-\bar{u}_0''\frac{\partial\bar{\psi}_1}{\partial\bar{x}}+\lambda^2\bar{u}_0\frac{\partial^3\bar{\psi}_1}{\partial\bar{x}^3}\right)=F_1\left(\lambda^4\frac{\partial^4\bar{\psi}_1}{\partial\bar{x}^4}+2\lambda^2\frac{\partial^4\bar{\psi}_1}{\partial\bar{x}^2\partial\bar{y}^2}+\frac{\partial^4\bar{\psi}_1}{\partial\bar{y}^4}\right)+\frac{3}{2}F_1'\left(\lambda^2\frac{\partial^3\bar{\psi}_1}{\partial\bar{x}^2\partial\bar{y}}+\frac{\partial^3\bar{\psi}_1}{\partial\bar{y}^3}\right)+\frac{1}{2}F_2''\left(\frac{\partial^2\bar{\psi}_1}{\partial\bar{y}^2}-\lambda^2\frac{\partial^2\bar{\psi}_1}{\partial\bar{x}^2}\right)$$

$$- \beta \left(\lambda^6 \frac{\partial^6 \bar{\psi}_1}{\partial \bar{x}^6} + 3\lambda^4 \frac{\partial^6 \bar{\psi}_1}{\partial \bar{x}^4 \partial \bar{y}^2} + 3\lambda^4 \frac{\partial^6 \bar{\psi}_1}{\partial \bar{x}^2 \partial \bar{y}^4} + \frac{\partial^6 \bar{\psi}_1}{\partial \bar{y}^6} \right).$$

Equation (3.17) is subject to the boundary conditions (3.15d) and (3.15e), which, in terms of the streamfunction $\bar{\psi}_1$, are

$$\left. \frac{\partial \bar{\psi}_1}{\partial \bar{y}} \right|_{\bar{y}=\pm 1} = \mp \bar{u}_0'(\pm 1) \sin(2\pi \bar{x}) \tag{3.18}$$

and

$$\left. \frac{\partial \bar{\psi}_1}{\partial \bar{x}} \right|_{\bar{y}=\pm 1} = 0. \tag{3.19}$$

Equation (3.17) is also subject to the higher order boundary condition (3.15f), which, in terms of $\bar{\psi}_1$, becomes

$$- \lambda^2 \frac{\partial^2 \bar{\psi}_1}{\partial \bar{x}^2 \partial \bar{y}} + \frac{\partial^3 \bar{\psi}_1}{\partial \bar{y}^3} = 0, \text{ at } \bar{y} = \pm 1. \tag{3.20}$$

Because of the form of the boundary condition (3.18), the linearity of (3.17), and the fact that the coefficients in (3.17) are independent of $\bar{x}$, we seek a solution to (3.17), subject to the boundary conditions (3.18), (3.19), and (3.20), in the form

$$\bar{\psi}_1(\bar{x}, \bar{y}) = \Psi_1(\bar{y}) \cos(2\pi \bar{x}) + \Psi_2(\bar{y}) \sin(2\pi \bar{x}). \tag{3.21}$$

Upon substituting (3.21) into (3.17), as well as the boundary conditions (3.18), (3.19), and (3.20), and collecting the terms multiplying $\cos(2\pi\bar{x})$ and $\sin(2\pi\bar{x})$, the following boundary-value problems for Ψ_1 and Ψ_2 are obtained:

$$\begin{aligned} 2\pi R_e \lambda \left[\bar{u}_0 \Psi_2'' - \left(\bar{u}_0'' + 4\pi^2 \lambda^2 \bar{u}_0 \right) \Psi_2 \right] \\ = F_1 \left(16\pi^4 \lambda^4 \Psi_1 - 8\pi^2 \lambda^2 \Psi_1'' + \Psi_1'''' \right) \\ - \frac{3}{2} F_1' \left(6\pi^2 \lambda^2 \Psi_1' - \Psi_1''' \right) + \frac{1}{2} F_1'' \left(\Psi_1'' + 4\pi^2 \lambda^2 \Psi_1 \right) \\ + \beta \left(64\pi^6 \lambda^6 \Psi_1 - 48\pi^4 \lambda^4 \Psi_1'' + 12\pi^2 \lambda^4 \Psi_1'''' - \Psi_1^{(6)} \right), \end{aligned} \tag{3.22a}$$

$$\begin{aligned} 2\pi R_e \lambda \left[(\bar{u}_0'' + 4\pi^2 \lambda^2 \bar{u}_0) \Psi_1 - \bar{u}_0 \Psi_1'' \right] \\ = F_1 \left(16\pi^4 \lambda^4 \Psi_2 - 8\pi^2 \lambda^2 \Psi_2'' + \Psi_2'''' \right) \end{aligned} \tag{3.22b}$$

$$-\frac{3}{2}F_1'\left(6\pi^2\lambda^2\Psi_2' - \Psi_2'''\right) + \frac{1}{2}F_1''\left(\Psi_2'' + 4\pi^2\lambda^2\Psi_2\right)$$
$$+\beta\left(64\pi^6\lambda^6\Psi_2 - 48\pi^4\lambda^4\Psi_2'' + 12\pi^2\lambda^4\Psi_2'''' - \Psi_2^{(6)}\right),$$

$$\Psi_1(\pm1) = 0 \quad \text{and} \quad \Psi_2(\pm1) = 0, \tag{3.22c}$$

$$\Psi_1'(\pm1) = 0 \quad \text{and} \quad \Psi_2'(\pm1) = \mp\bar{u}_0'(\pm1), \tag{3.22d}$$

$$\Psi_1'''(\pm1) = 0 \quad \text{and} \quad \Psi_2'''(\pm1) = \pm4\pi^2\lambda^2\bar{u}_0'(\pm1). \tag{3.22e}$$

We have computed approximate solutions for Ψ_1 and Ψ_2 with `NDSolve` in *Mathematica*, and combined the computed solution with (3.21) to find the streamfunction $\bar{\psi}_1$. From the dimensionless solution (3.2) for a linear bipolar fluid in a flat walled channel, the corresponding streamfunction is obtained in the form

$$\bar{\psi}_0(\bar{y}) = \frac{1}{2}\left(\bar{y} - \frac{1}{3}\bar{y}^3\right) - \beta\left(\bar{y} - \sqrt{\beta}\,\mathrm{sech}\left(\frac{1}{\sqrt{\beta}}\right)\sinh\left(\frac{\bar{y}}{\sqrt{\beta}}\right)\right). \tag{3.23}$$

Therefore, the streamfunction, $\bar{\psi}$, up to first order in $\bar{\delta}$, is $\bar{\psi} = \bar{\psi}_0 + \delta\bar{\psi}_1$, where $\bar{\psi}_0$ is given by (3.23) for the bipolar fluid (both linear and nonlinear).

4. Perturbation expansion in λ

In this section we seek a solution to the various boundary-value problems for the flow of a fluid in a sinusoidally constricted channel using a regular perturbation expansion in the parameter $\lambda = \frac{y_0}{L}$. We assume throughout that $\lambda \ll 1$. The advantage of using λ as the parameter in the perturbation expansion, as opposed to $\bar{\delta}$, is that we are able to obtain closed form solutions. The disadvantage is that to obtain these closed form solutions we must assume that the viscosity is constant. Thus, we assume throughout that $\alpha = 0$. This technique has been applied in [6] for a Newtonian fluid in a sinusoidally constricted pipe.

We introduce the streamfunction $\bar{\psi}$ defined by

$$\bar{u} = \frac{\partial\bar{\psi}}{\partial\bar{y}} \quad \text{and} \quad \bar{v} = -\frac{\partial\bar{\psi}}{\partial\bar{x}}, \tag{4.1}$$

and seek a solution of the form

$$\bar{\psi} = \bar{\psi}_0 + \lambda\bar{\psi}_1 + O(\lambda^2). \tag{4.2}$$

Upon applying the definition in (4.1), and the assumption (4.2), to the dimensionless boundary-value problem (2.15), a straightforward calculation yields, up to first order in λ, the following boundary-value problems:

Linear Bipolar Zeroth Order:

$$\frac{\partial^4 \bar{\psi}_0}{\partial \bar{y}^4} - \beta \frac{\partial^6 \bar{\psi}_0}{\partial \bar{y}^6} = 0, \text{ in } \Omega_\delta, \tag{4.3a}$$

$$\frac{\partial \bar{\psi}_0}{\partial \bar{y}} = \frac{\partial \bar{\psi}_0}{\partial \bar{x}} = 0, \text{ at } \bar{y} = \pm \bar{y}_{\bar{\delta}}(\bar{x}), \tag{4.3b}$$

$$\frac{\partial^3 \bar{\psi}_0}{\partial \bar{y}^3} = 0, \text{ at } \bar{y} = \pm \bar{y}_{\bar{\delta}}(\bar{x}). \tag{4.3c}$$

Linear Bipolar First Order:

$$\frac{\partial^4 \bar{\psi}_1}{\partial \bar{y}^4} - \beta \frac{\partial^6 \bar{\psi}_1}{\partial \bar{y}^6} = R_e \left(\frac{\partial \bar{\psi}_0}{\partial \bar{y}} \frac{\partial^3 \bar{\psi}_0}{\partial \bar{y}^2 \partial \bar{x}} - \frac{\partial \bar{\psi}_0}{\partial \bar{x}} \frac{\partial^3 \bar{\psi}_0}{\partial \bar{y}^3} \right), \text{ in } \Omega_\delta, \tag{4.4a}$$

$$\frac{\partial \bar{\psi}_1}{\partial \bar{y}} = \frac{\partial \bar{\psi}_1}{\partial \bar{x}} = 0, \text{ at } \bar{y} = \pm \bar{y}_{\bar{\delta}}(\bar{x}), \tag{4.4b}$$

$$\frac{\partial^3 \bar{\psi}_1}{\partial \bar{y}^3} = 0, \text{ at } \bar{y} = \pm \bar{y}_{\bar{\delta}}(\bar{x}). \tag{4.4c}$$

The equivalent boundary-value problems for a Newtonian fluid follow from (4.3) and (4.4), respectively, upon setting $\beta = 0$ and dropping the higher-order boundary conditions (4.3c) and (4.4c).

The solution to the boundary-value problem (4.3) involves a straightforward, but lengthy calculation. We find that the solution to (4.3), which has the same constant volumetric flow rate as the streamfunction for a Newtonian fluid with $\bar{\delta}$ the perturbation parameter (i.e. the streamfunction (3.23) with $\beta = 0$) is

$$\bar{\psi}_0(\bar{x}, \bar{y}) = \frac{\bar{y}^3 + 6\beta\bar{y} - 6\beta^{3/2} \operatorname{sech}\left(\frac{\bar{y}_{\bar{\delta}}(\bar{x})}{\sqrt{\beta}}\right) \sinh\left(\frac{\bar{y}}{\sqrt{\beta}}\right) - 3\bar{y}_{\bar{\delta}}^2(\bar{x})\bar{y}}{6[3\beta\bar{y}_{\bar{\delta}}(\bar{x}) - \bar{y}_{\bar{\delta}}^3(\bar{x}) - 3\beta^{3/2} \tanh\left(\frac{\bar{y}_{\bar{\delta}}(\bar{x})}{\sqrt{\beta}}\right)]}. \tag{4.5}$$

Upon substituting $\bar{\psi}_0$, as given by equation (4.5), into the boundary-value problem (4.4), we are able to compute, with the aid of *Mathematica*, a closed form solution to (4.4) with the same volumetric flow rate, up to first order in λ, as $\bar{\psi}_0$. The full solution, which is given in Appendix C of the thesis [16], is reproduced in Appendix A of this paper.

5. Results

5.1. Perturbation expansion in $\bar{\delta}$

Various plots of the flow based on the perturbation expansion in $\bar{\delta}$, for fluids with both a constant viscosity (i.e. Newtonian and linear bipolar) and a nonlinear viscosity (i.e. non-Newtonian and nonlinear bipolar), are presented below. The base values of the constants are taken to be $\alpha = 0.1$, $\varepsilon = 0.1s^{-2}$, $R_e = 1$, $\bar{\delta} = 0.1$, and $\lambda = 0.1$, except where noted otherwise. We also assume, for simplicity, that $\frac{U}{y_0} = 1$. Since the flow for both the nonlinear bipolar and linear bipolar fluids depend continuously on β, and converge to the flow for a non-Newtonian and Newtonian fluid, respectively, as $\beta \to 0^+$, the results for both a non-Newtonian and a Newtonian fluid correspond to those for a nonlinear bipolar and linear bipolar fluid, respectively, with $\beta = 0$. As the resulting boundary-value problem (3.22) in the domain perturbation method is posed on the domain $-1 \leq \bar{y} \leq 1$, we obtain information in the divergent portion of the channel, where $1 < |\bar{y}| < |\bar{y}_{\bar{\delta}}(\bar{x})|$, for $0 < \bar{x} < 1$, through polynomial extrapolation.

The effect of an increase in the parameter $\lambda = \frac{y_0}{L}$ on the dimensionless axial velocity profiles is shown in Figure 2 for fluids with a nonlinear viscosity. For $\beta = 0$, as λ is increased, the profiles in the divergent portion of the channel deviate from their parabolic shape near the boundary, with flow reversal occurring for $\lambda = 0.7$ in the peak of the channel. For $\beta > 0$ (with $\beta = 5$ shown), the profiles no longer vary with λ, and flow reversal does not occur. The profiles flatten as β is increased. Analogous results for fluids with a constant viscosity are similar.

The wall shear stress, to first approximation, is $\tau_w = \tau_{xy}|_{y=\pm y_\delta(x)}$, and is an important quantity to calculate in studies of blood flow as it is implicated in the initiation and progression of arterial disease [6]. For a nonlinear bipolar fluid, τ_w assumes the form

$$\tau_w = \left[\mu(|\mathbf{e}|)\frac{\partial u}{\partial y} - \mu_1\left(\frac{\partial^3 u}{\partial x^2 \partial y} + \frac{\partial^3 u}{\partial y^3} + \frac{\partial^3 v}{\partial x \partial y^2}\right)\right]\Bigg|_{y=\pm 1}. \tag{5.1}$$

In (5.1), we approximate the wall boundary $\bar{y} = \pm\bar{y}_{\bar{\delta}}(\bar{x})$ by $\bar{y} = \pm 1$, as in the domain perturbation method, and apply the boundary condition $\bar{v}_1(\bar{x}, \pm 1) = 0$. We define the dimensionless wall shear stress to be

$$\bar{\tau}_w = \frac{\tau_w}{G y_0}, \tag{5.2}$$

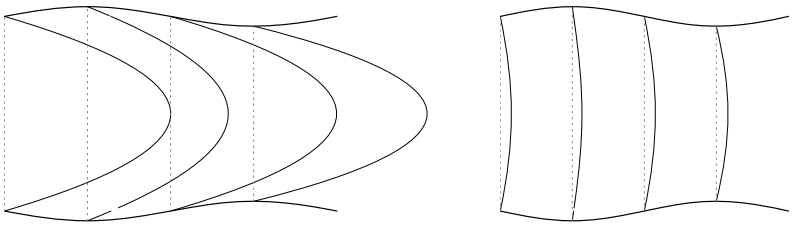

(a) $\lambda = 0.1,\ \beta = 0$ **(c)** $\lambda = 0.1,\ \beta = 5$

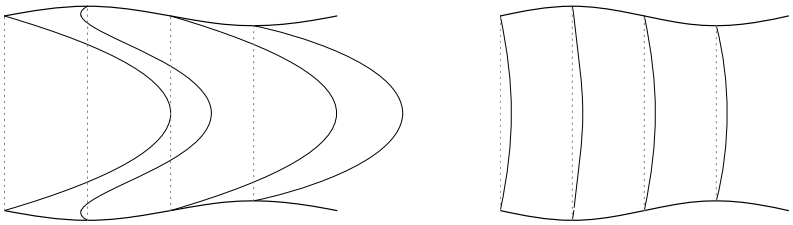

(b) $\lambda = 0.7,\ \beta = 0$ **(d)** $\lambda = 0.7,\ \beta = 5$

Figure 2: Nondimensional axial velocity profiles for fluids with a nonlinear viscosity over one period, L, of the wavy wall at $\bar{x} = 0$, $\bar{x} = \frac{1}{4}$, $\bar{x} = \frac{1}{2}$, and $\bar{x} = \frac{3}{2}$, for several values of β and λ. The common parameters in each model are taken to be $\alpha = 0.1$, $\varepsilon = 0.1$, $\bar{\delta} = 0.1$, and $R_e = 1$.

and convert (5.1) to dimensionless variables; this yields

(5.3)
$$\bar{\tau}_w = \left[(1+\varepsilon^{-1}|\mathbf{e}|^2)^{-\alpha/2}\frac{\partial \bar{u}}{\partial \bar{y}} - \beta\left(\lambda^2\frac{\partial^3 \bar{u}}{\partial \bar{x}^2 \partial \bar{y}} + \frac{\partial^3 \bar{u}}{\partial \bar{y}^3} + \lambda^2\frac{\partial^3 \bar{v}}{\partial \bar{x}\partial \bar{y}^2}\right)\right]\Bigg|_{\bar{y}=\pm 1}.$$

Figure 3 shows plots of $\bar{\tau}_w$ for an increasing sequence of α, for the non-Newtonian and nonlinear bipolar fluid, respectively. In Figure 3(a), $\alpha = 0$ corresponds to the Newtonian fluid, while in Figure 3(b), $\alpha = 0$ corresponds to the linear bipolar fluid. In each case, the effect of α is to increase the values of $\bar{\tau}_w$, with $\bar{\tau}_w$ remaining negative for each α. For the non-Newtonian fluid, as α is increased, the amplitude of $\bar{\tau}_w$ decreases, with $\bar{\tau}_w$ becoming almost constant for $\alpha = 0.9$. The amplitude of $\bar{\tau}_w$ also decreases for a bipolar fluid, however, the rate of this decrease is slowed. At $\alpha = 0.9$, $\bar{\tau}_w$ still varies along the channel in a sinusoidal fashion similar to the variation when $\alpha = 0$.

The dimensionless wall shear stress, $\bar{\tau}_w$, is shown for an increasing sequence of λ, for the non-Newtonian and nonlinear bipolar fluid in Figure 4.

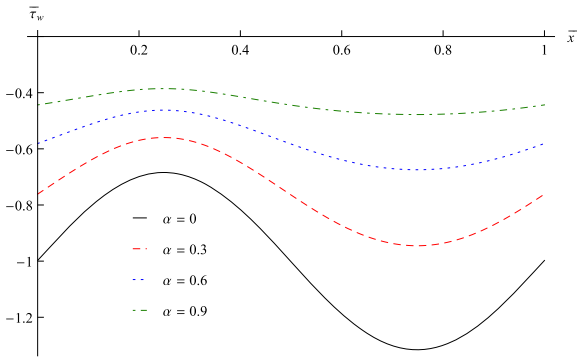

(a) $\beta = 0$

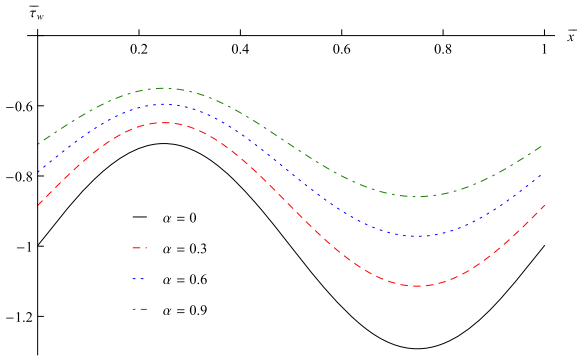

(b) $\beta = 0.1$

Figure 3: The nondimensional wall shear stress, $\bar{\tau}_w$, at the upper wall, $\bar{y} = 1$, for the non-Newtonian and nonlinear bipolar fluids, respectively, for several values of α. The common parameters in each model are taken to be $\bar{\delta} = 0.1$, $\lambda = 0.1$, and $R_e = 1$.

A bifurcation between the fluid models occurs in the behavior of $\bar{\tau}_w$ as λ is increased. For $\beta = 0$ (Newtonian and non-Newtonian), $\bar{\tau}_w$ follows the variation in the wavy wall, with the amplitude increasing with λ, but always remaining negative. For $\beta > 0$ (linear bipolar and bipolar), $\bar{\tau}_w$ again follows the variation in the wavy wall as λ is increased, but the increase in amplitude is greater than for the case with $\beta = 0$, with $\bar{\tau}_w$ assuming positive values in the divergent portion of the channel for $\lambda = 0.5$ and 0.7.

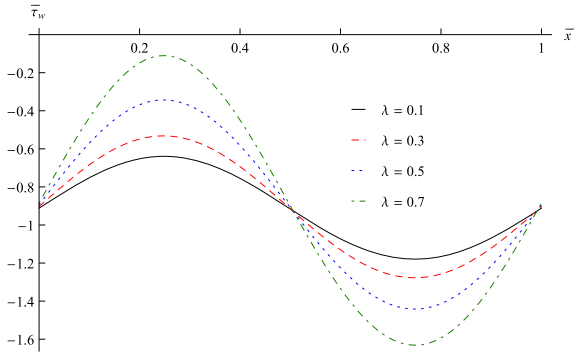

(a) $\beta = 0$

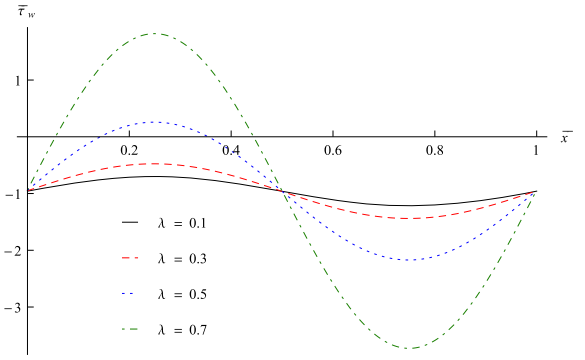

(b) $\beta = 0.1$

Figure 4: The nondimensional wall shear stress, $\bar{\tau}_w$, for the non-Newtonian and nonlinear bipolar fluids at the upper wall, $\bar{y} = 1$, for various values of λ and for $\alpha = 0.1$, $\varepsilon = 0.1$, $R_e = 1$, and $\bar{\delta} = 0.1$.

The vorticity, ξ, for a 2-D flow is given by

$$\xi = \frac{\partial v}{\partial x} - \frac{\partial u}{\partial y}. \tag{5.4}$$

We take $\Xi = \frac{Gy_0}{\mu_0}$ as the characteristic vorticity, so that the dimensionless vorticity is given by

$$\bar{\xi} = \frac{\xi}{\Xi} = \lambda^2 \frac{\partial \bar{v}}{\partial \bar{x}} - \frac{\partial \bar{u}}{\partial \bar{y}}. \tag{5.5}$$

We can characterize flow separation, in a first approximation, as occurring when the dimensionless vorticity is zero at the channel wall.

The contour lines of the vorticity for an increasing sequence of λ are shown in Figures 5 for the Newtonian, non-Newtonian, and nonlinear bipolar fluids. The non-Newtonian fluid exhibits a change in behavior from the Newtonian as λ increases. Circular contours emanate from the divergent portion of the channel, separating the contours which approach the boundary, and for $\lambda = 0.7$, a zero contour occurs in the peak of the channel wall, which implies flow separation. The occurrence of flow separation is significant because it occurs for only $R_e = 1$ and a slight constriction. As noted by Hemmat and Borhan [10], there is a debate in the literature on the occurrence of flow separation at low Reynolds numbers, with some studies, e.g. [6], reporting no flow separation below $R_e = 25$, while others, e.g. [9], indicate that the possibility occurs at lower Reynolds numbers. For $\beta > 0$, both for the linear bipolar fluid (not shown) and the nonlinear bipolar fluid, a change in behavior from the non-Newtonian fluid occurs as λ increases. In each case, the contours flatten out in the divergent portion of the channel, but no flow separation is observed.

5.2. Perturbation expansion in λ

Various plots of the flow for the asymptotic solutions found for the perturbation expansion in λ, for both the Newtonian fluid and the linear bipolar fluid, are presented below. As in the previous section, we refer to results for a Newtonian fluid with $\beta = 0$. We note that we observe no significant differences between the Newtonian and linear bipolar fluids at low Reynolds numbers; our results are for moderate and high Reynolds numbers.

In Figure 6, representative flow patterns for the streamlines $\bar{\psi} \equiv constant$, to first order in λ, are shown for increasing β, with $\bar{\delta} = 0.3$, $\lambda = 0.1$, and $R_e = 600$. For the Newtonian fluid, Figure 6(a), the streamlines follow the variation in the channel wall with a region of circulation behind the trough of the wall, corresponding to flow separation, while a circular streamline encloses the centerline of the channel prior to the trough of the wall. For a linear bipolar fluid, the μ_1 parameter, or in nondimensional form, the $\beta = \frac{\mu_1}{\mu_0 y_0^2}$ parameter, corresponds to a stronger mechanism of dissipation. This is observed in Figures 6(b)–(d) in which $\beta > 0$. In Figure 6(b), $\beta = 0.01$ and the streamlines are qualitatively similar to the case for which $\beta = 0$, but the circular regions have decreased slightly. As β is increased to 0.1, in Figure 6(c), the circular streamline about the centerline disappears, while a

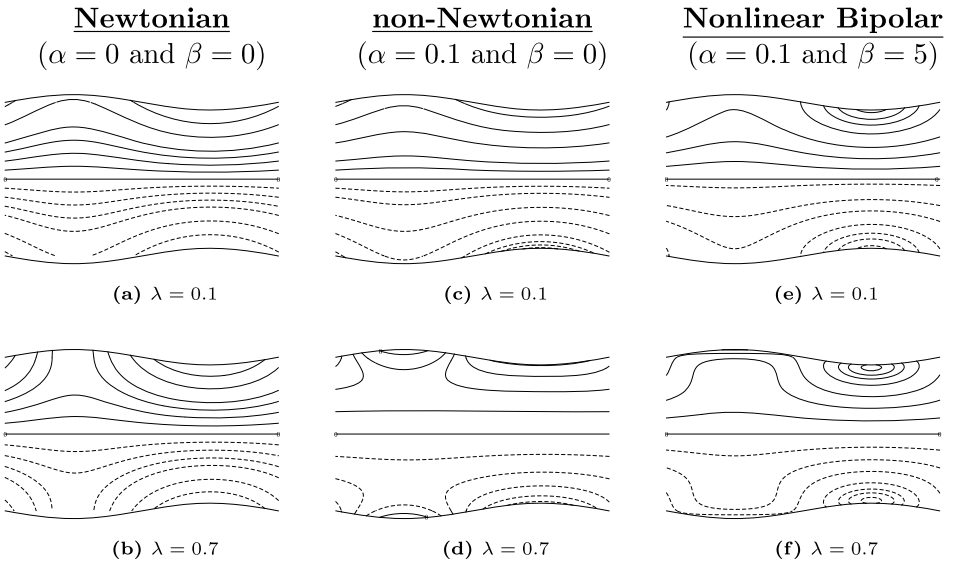

Figure 5: Contour lines of the vorticity for fluids with a nonlinear viscosity with several different values of λ and β. The common parameters in each model are taken to be $\alpha = 0.1$, $\varepsilon = 0.1$, $\bar{\delta} = 0.1$, and $R_e = 1$. Solid lines correspond to positive vorticity and dashed lines correspond to negative vorticity.

small circulation region remains behind the trough of the wall. This result is most similar to those observed in [9] for the flow of a Newtonian fluid in a wavy tube with $R_e = 600$. As β is increased further to 0.2, Figure 6(d), the streamlines follow the variation in the channel wall and no circulation occurs.

Dimensionless axial velocity profiles are shown in Figure 7 at several locations along the channel, over a range of β, for $\bar{\delta} = 0.5$, $\lambda = 0.1$, and $R_e = 150$. Two points are of particular interest as β is increased: $\bar{x} = 0$ and $1/2$. At $\bar{x} = 0$, for $\beta = 0$, flow reversal occurs near the channel wall, as also noted by Chow and Soda [6] for a Newtonian fluid in a wavy tube. As β is increased from zero, this behavior no longer occurs. For $\beta = 0.01$, the profiles are flat as they approach the wall, but no reversal occurs, while for $\beta = 0.1$ and 0.2, the profiles assume their familiar parabolic shape, which occurs for lower values of R_e or $\bar{\delta}$. At $\bar{x} = 1/2$, for both $\beta = 0$ and 0.1, the profiles do not have a parabolic shape and the maximum velocity no longer occurs at the centerline of the channel. Such profiles were predicted by Forrester and Young [9] and Chow and Soda [6] for a Newtonian fluid

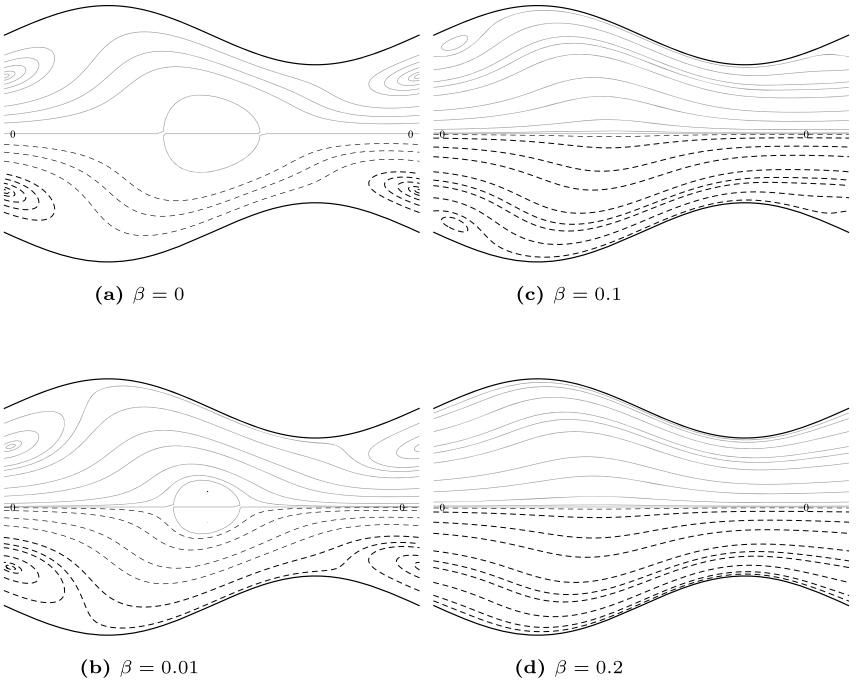

(a) $\beta = 0$ **(c)** $\beta = 0.1$

(b) $\beta = 0.01$ **(d)** $\beta = 0.2$

Figure 6: Streamlines $\bar{\psi} = \bar{\psi}_0 + \lambda\bar{\psi}_1 \equiv constant$ for four different values of β with $\alpha = 0$ and for $\bar{\delta} = 0.3$, $\lambda = 0.1$ and $R_e = 600$. Solid lines correspond to positive streamlines and dashed lines correspond to negative streamlines.

at the corresponding location in a wavy tube. As β is increased to 0.1 and, subsequently, 0.2, the profiles revert to a parabolic shape and the maximum velocity occurs along the centerline.

Similar behavior is also seen in Figure 8, which shows the dimensionless axial velocity profiles for an increase in $\bar{\delta}$, for both $\beta = 0$ and $\beta = 0.1$. At a small constriction (not shown), the profiles for the Newtonian and linear bipolar fluid are indistinguishable. As $\bar{\delta}$ is increased to 0.3 the profiles for a Newtonian fluid flatten out and, subsequently, exhibit flow reversal near the wall at $\bar{x} = 0$, while the maximum velocity no longer occurs along the centerline at $\bar{x} = 1/2$. At the same time, the corresponding profiles for the linear bipolar fluid only deviate slightly from their parabolic shape. At $\bar{\delta} = 0.7$ for the linear bipolar fluid, the maximum velocity no longer occurs at the centerline at $\bar{x} = 1/2$, while a very weak flow reversal occurs in the corresponding profile for a Newtonian fluid.

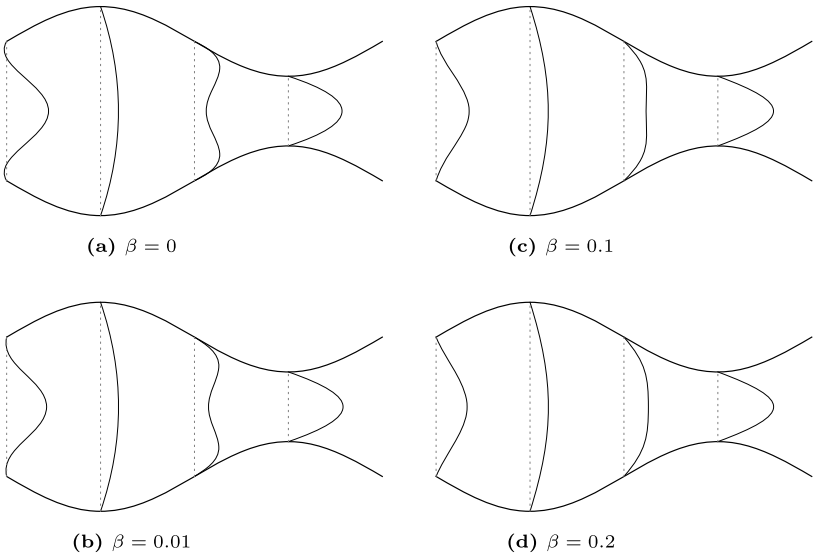

(a) $\beta = 0$ **(c)** $\beta = 0.1$

(b) $\beta = 0.01$ **(d)** $\beta = 0.2$

Figure 7: Nondimensional axial velocity profiles over one period, L, of the wavy wall at $\bar{x} = 0$, $\bar{x} = \frac{1}{4}$, $\bar{x} = \frac{1}{2}$, and $\bar{x} = \frac{3}{2}$, for several values of β with $\alpha = 0$. The common parameters in each model are taken to be $\bar{\delta} = 0.5$, $\lambda = 0.1$ and $R_e = 150$.

The wall shear stress for the linear bipolar fluid, with the boundary taken at $y = \pm\bar{y}_{\bar{\delta}}(x)$ (and not approximated at $y = \pm y_0$, as in (5.1)) is, to first approximation,

(5.6)
$$\tau_w = \left[\mu_0\left(\frac{\partial u}{\partial y} + \frac{\partial v}{\partial x}\right) - \mu_1\left(\frac{\partial^3 u}{\partial x^2 \partial y} + \frac{\partial^3 u}{\partial y^3} + \frac{\partial^3 v}{\partial x^3} + \frac{\partial^3 v}{\partial x \partial y^2}\right)\right]\Bigg|_{y=\pm y_\delta(x)}.$$

Converting (5.6) to dimensionless variables, as in (5.3), we find that, to first order in λ

$$\bar{\tau}_w = \left[\frac{\partial \bar{u}}{\partial \bar{y}} - \beta\frac{\partial^3 \bar{u}}{\partial \bar{y}^3}\right]\Bigg|_{\bar{y}=\pm\bar{y}_{\bar{\delta}}(\bar{x})}. \tag{5.7}$$

In Figure 9, the nondimensional wall shear stress is plotted over one period of the wavy wall for several values of β, with $\bar{\delta} = 0.4$, $\lambda = 0.1$, and $R_e = 150$. As β is increased, $\bar{\tau}_w$ decreases slightly in the peak of the channel, and by an order of magnitude in the trough. This slight decrease in the peak of the

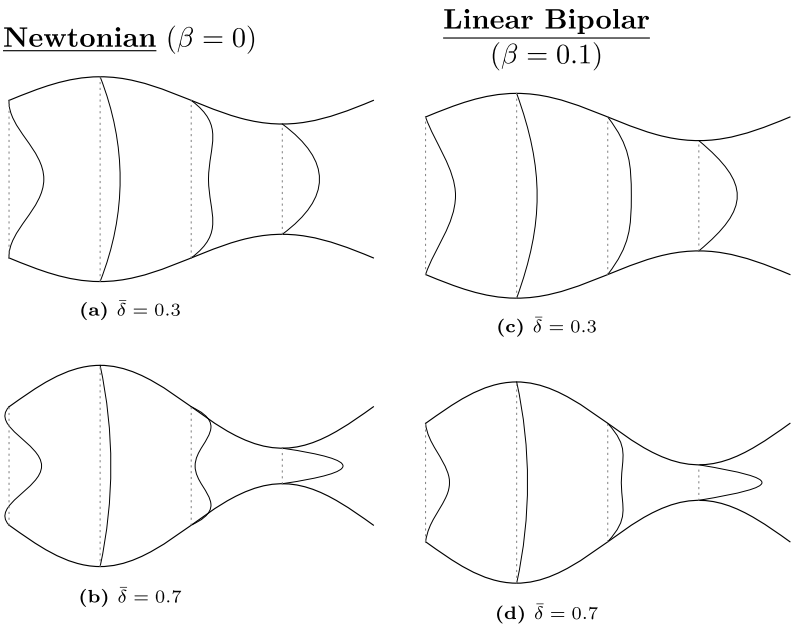

Figure 8: Nondimensional axial velocity profiles over one period, L, of the wavy wall at $\bar{x} = 0$, $\bar{x} = \frac{1}{4}$, $\bar{x} = \frac{1}{2}$, and $\bar{x} = \frac{3}{2}$, for several values of β and $\bar{\delta}$ with $\alpha = 0$. The common parameters in each model are taken to be $\lambda = 0.1$ and $R_e = 150$.

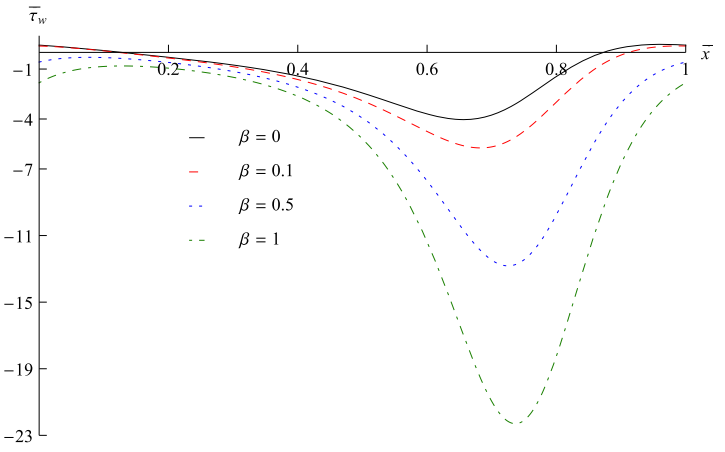

Figure 9: The nondimensional wall shear stress at the upper wall, $\bar{\tau}_w(\bar{x}, \bar{y}_{\bar{\delta}}(\bar{x}))$, for various values of β with $\alpha = 0$ and for $\bar{\delta} = 0.4$, $\lambda = 0.1$, and $R_e = 150$.

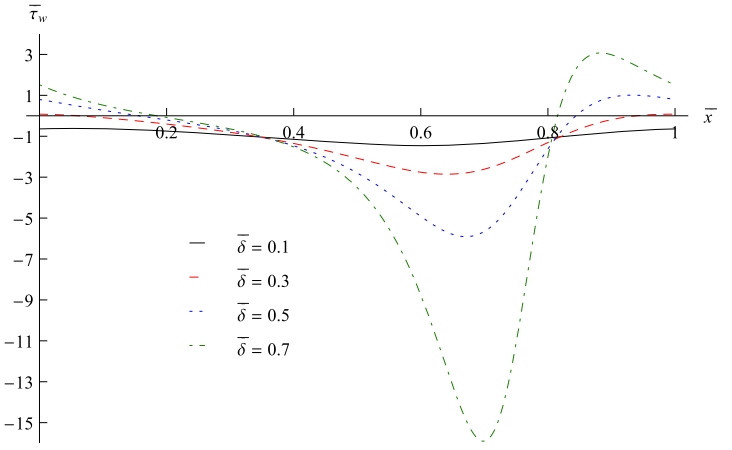

(a) $\beta = 0$

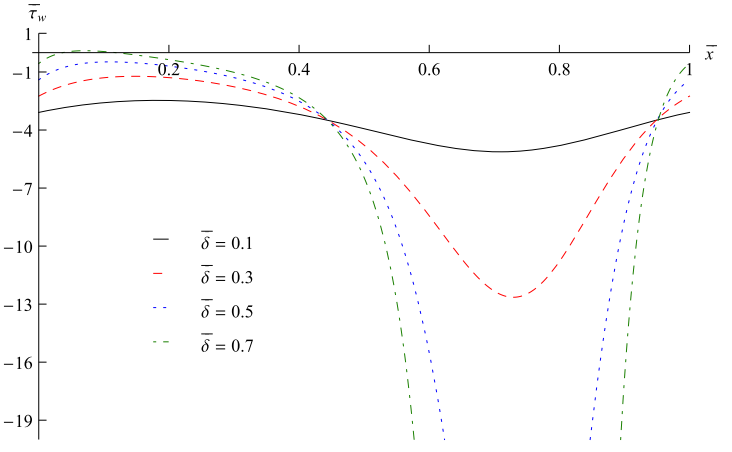

(b) $\beta = 1$

Figure 10: The nondimensional wall shear stress at the upper wall, $\bar{\tau}_w(\bar{x}, \bar{y}_{\bar{\delta}}(\bar{x}))$, for the Newtonian and linear bipolar fluids for various values of $\bar{\delta}$ and for $\alpha = 0$, $\lambda = 0.1$, and $R_e = 150$.

channel causes $\bar{\tau}_w$ to remain negative throughout the channel for $\beta = 0.5$ and 1, while for $\beta = 0$ and 0.1, $\bar{\tau}_w$ is positive in the peak and trough of the channel, respectively, indicating possible flow separation; this behavior is further illustrated in Figure 10, which shows the dimensionless wall shear stress for an increasing sequence of $\bar{\delta}$, for the Newtonian and linear bipolar fluids, respectively, with $\lambda = 0.1$ and $R_e = 150$. For a Newtonian fluid, $\bar{\tau}_w$

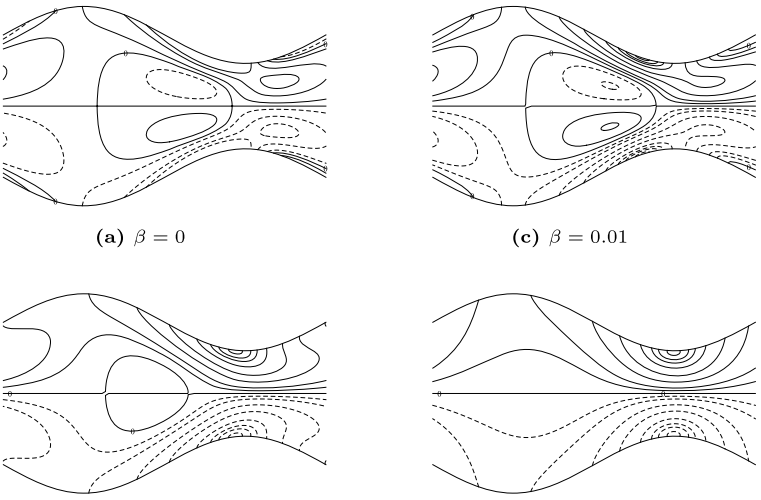

(a) $\beta = 0$ **(c)** $\beta = 0.01$

(b) $\beta = 0.1$ **(d)** $\beta = 1$

Figure 11: Contour lines of the dimensionless vorticity for several different values of β with $\alpha = 0$, $\bar{\delta} = 0.4$, $\lambda = 0.1$ and $R_e = 200$. Solid lines correspond to positive vorticity and dashed lines correspond to negative vorticity.

assumes positive values in the peak and trough of the channel; however, for a linear bipolar fluid, $\bar{\tau}_w$ remains negative except in the peak of the channel for $\bar{\delta} = 0.7$. These differences in $\bar{\tau}_w$, between the Newtonian and the linear bipolar fluid, persist if, instead, we fix $\bar{\delta} = 0.4$, and take an increasing sequence of R_e.

From equation (5.5), the dimensionless vorticity, to first order in λ, is given by $\bar{\xi} = -\frac{\partial \bar{u}}{\partial \bar{y}}$ and we may characterize flow separation (in a first approximation) as occurring when the dimensionless vorticity is zero on the channel wall. In Figure 11, contour lines of the dimensionless vorticity are shown for increasing β, with $\bar{\delta} = 0.4$, $\lambda = 0.1$, and $R_e = 200$. For $\beta = 0$ and 0.01, possible flow separation occurs just prior to the peak of the channel. As β is further increased to 0.1 and 1, the contour lines converge to those seen at lower Reynolds numbers or for channels with less severe constrictions.

The differences in the vorticity contours between the Newtonian fluid and the linear bipolar fluid are further illustrated in Figure 12, in which the contour lines of the dimensionless vorticity are shown for an increasing channel constriction, with $\lambda = 0.1$ and $R_e = 100$, for both the Newtonian fluid and the linear bipolar fluid, with $\beta = 0.1$. For a small constriction, $\bar{\delta} = 0.1$ and the contour lines for each model are nearly identical. At $\bar{\delta} = 0.3$,

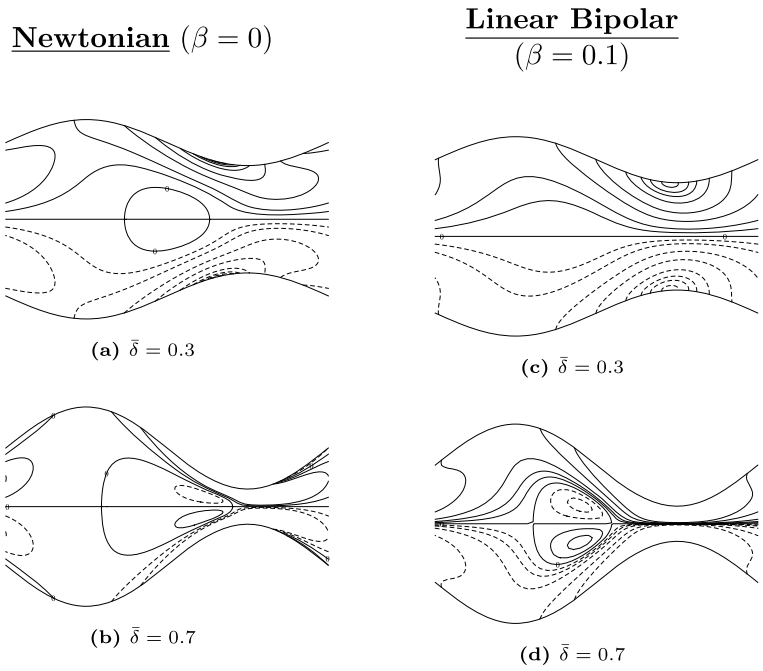

Figure 12: Contour lines of the dimensionless vorticity for several different values of $\bar{\delta}$ and β with $\alpha = 0$, $\lambda = 0.1$, and $R_e = 100$. Solid lines correspond to positive vorticity and dashed lines correspond to negative vorticity.

the contour lines for the models begin to diverge slightly, with flow separation occurring for the Newtonian model at $\bar{\delta} = 0.5$ (not shown), but not for the linear bipolar fluid model, even for $\bar{\delta} = 0.7$.

6. Summary

For the approach with $\bar{\delta}$ as the perturbation parameter, in Section 3, significant qualitative differences between the non-Newtonian fluid and the nonlinear bipolar fluid exist. Flow separation, and subsequent reattachment, is observed in the divergent portion of the channel for the non-Newtonian fluid, but not for the nonlinear bipolar fluid, with $\lambda = 0.7$ at low Reynolds number and mild constriction. As μ_1, or equivalently, β, is increased from zero, the axial velocity profiles flatten from their parabolic shape. The wall shear stress varies with the Reynolds number for the non-Newtonian fluid, but not for the nonlinear bipolar fluid. For $\lambda > 0.5$, a large change in amplitude of the wall shear stress occurs, which causes a sign change, for the

Table 1: Parameter values for which the non-Newtonian and the nonlinear bipolar fluid diverge for the corresponding flow characteristic. In each case, $\bar{\delta} = 0.1$, $\alpha = 0.1$, and $\varepsilon = 0.1$

	non-Newtonian ($\alpha > 0$, $\beta = 0$)	**Nonlinear Bipolar** ($\alpha > 0$, $\beta > 0$)
Flow Separation	• Occurs at $\lambda = 0.7$ and $R_e = 1$	• None observed
Shear Stress	• Amplitude varies proportionally with R_e	• no variation with R_e
	• Remains negative for $0.1 \leq \lambda \leq 0.7$	• Turns positive for $0.5 \leq \lambda \leq 0.7$ • Decreases for $\beta > 0$
Vorticity	• Zero contour near peak of wall for $0.5 \leq \lambda \leq 0.7$	• Contours flatten in peak of channel for $0.5 \leq \lambda \leq 0.7$
Axial Velocity Profiles	• Parabolic in shape	• Profiles flatten as $\beta \uparrow$

nonlinear bipolar fluid, while only a moderate change in amplitude, with no sign change, occurs for the non-Newtonian fluid. Finally, the wall shear stress decreases as β is increased from zero. See Table 1 for a summary of these differences.

When λ is the perturbation parameter, as in Section 4, several significant qualitative differences between the linear bipolar fluid and the Newtonian fluid occur. Flow separation, which occurs at high Reynolds numbers and moderate constriction for the Newtonian fluid, does not occur for the linear bipolar for all β greater than some critical positive number which depends upon the Reynolds number. A significant decrease occurs in the wall shear stress for $\beta > 1$. Furthermore, as β is increased from zero, the axial velocity profiles flatten from their parabolic shape, and the vorticity contours return to those seen at low Reynolds numbers or with a mild constriction. See Table 2 for a summary of these differences.

Appendix A. First order in λ streamfunction

The solution to the boundary-value problem (4.4), with $\psi_0(\bar{x}, \bar{y})$ given by (4.5), is

$$\psi_1(\bar{x},\bar{y}) = (R_e \operatorname{sech}\left[\frac{\bar{y}_{\bar{\delta}}(\bar{x})}{\sqrt{\beta}}\right](2(8\beta\cosh\left[\frac{\bar{y}_{\bar{\delta}}(\bar{x})}{\sqrt{\beta}}\right]\left(315\bar{y}\beta^2(6\bar{y}^2+209\beta)\cosh\left[\frac{\bar{y}}{\sqrt{\beta}}\right]\right.$$
$$\left. + 2\bar{y}(\bar{y}^6+42\bar{y}^4\beta+25200\beta^3)\cosh\left[\frac{\bar{y}_{\bar{\delta}}(\bar{x})}{\sqrt{\beta}}\right] - 105\beta^{3/2}(\bar{y}^4+147\bar{y}^2\beta+1107\beta^2)\right.$$

Table 2: Parameter values for which the linear bipolar fluid diverges from the Newtonian fluid for the corresponding flow characteristic. In each case, $\lambda = 0.1$

	Newtonian ($\alpha = 0$, $\beta = 0$)	**Linear Bipolar** ($\alpha = 0$, $\beta > 0$)
Streamlines	• Large circulation region prior to peak of wall for large R_e (≥ 600)	• Circulation region dissipates, disappears as $\beta \uparrow$ for large R_e (≥ 600)
Flow Separation	• occurs for $R_e = R_e^*$, for some $R_e^* = R_e^*(\bar{\delta}) > 0$	• Does not occur when $\beta > \beta^*$, for some $\beta^* = \beta^*(R_e) > 0$
Shear Stress	• Sign change near peak/trough of wall for $\bar{\delta} \geq 0.3$.	• Significant decrease for $\beta > 1$; can cause $\lvert\bar{\tau}_w\rvert > 0$, $\forall x$.
Vorticity	• Zero contour near peak/trough of wall and large circular zero contour about center of channel for moderate R_e (≥ 125).	• Contours return to those seen at low R_e or small $\bar{\delta}$ as $\beta \uparrow$.
Axial Velocity Profiles	• Flow reversal near walls for moderate R_e (150) • max does not occur along centerline for moderate R_e and $\bar{\delta} \geq 0.3$.	• Profiles flatten as $\beta \uparrow$

$$
\times \sinh\left[\frac{\bar{y}}{\sqrt{\beta}}\right]\Bigg) \sinh\left[\frac{\bar{y}_{\bar{\delta}}(\bar{x})}{\sqrt{\beta}}\right]^2 + 42\beta^{3/2} \sinh\left[\frac{\bar{y}_{\bar{\delta}}(\bar{x})}{\sqrt{\beta}}\right] \Bigg(20\bar{y}\beta(2\bar{y}^2 + 93\beta)\cosh\left[\frac{\bar{y}}{\sqrt{\beta}}\right]
$$

$$
+ 10\bar{y}\beta(2\bar{y}^2 + 93\beta)\cosh\left[\frac{\bar{y} - 2\bar{y}_{\bar{\delta}}(\bar{x})}{\sqrt{\beta}}\right] + 6\bar{y}^5 \cosh\left[\frac{\bar{y}_{\bar{\delta}}(\bar{x})}{\sqrt{\beta}}\right] + 3600\bar{y}\beta^2 \cosh\left[\frac{\bar{y}_{\bar{\delta}}(\bar{x})}{\sqrt{\beta}}\right]
$$

$$
+ 2\bar{y}^5 \cosh\left[\frac{3\bar{y}_{\bar{\delta}}(\bar{x})}{\sqrt{\beta}}\right] - 720\bar{y}\beta^2 \cosh\left[\frac{3\bar{y}_{\bar{\delta}}(\bar{x})}{\sqrt{\beta}}\right] + 20\bar{y}^3\beta \cosh\left[\frac{\bar{y} + 2\bar{y}_{\bar{\delta}}(\bar{x})}{\sqrt{\beta}}\right]
$$

$$
+ 930\bar{y}\beta^2 \cosh\left[\frac{\bar{y} + 2\bar{y}_{\bar{\delta}}(\bar{x})}{\sqrt{\beta}}\right] - 420\bar{y}^2\beta^{3/2} \sinh\left[\frac{\bar{y}}{\sqrt{\beta}}\right] - 2850\beta^{5/2} \sinh\left[\frac{\bar{y}}{\sqrt{\beta}}\right]
$$

$$
- 210\bar{y}^2\beta^{3/2} \sinh\left[\frac{\bar{y} - 2\bar{y}_{\bar{\delta}}(\bar{x})}{\sqrt{\beta}}\right] - 1875\beta^{5/2} \sinh\left[\frac{\bar{y} - 2\bar{y}_{\bar{\delta}}(\bar{x})}{\sqrt{\beta}}\right]
$$

$$
- 210\bar{y}^2\beta^{3/2} \sinh\left[\frac{\bar{y} + 2\bar{y}_{\bar{\delta}}(\bar{x})}{\sqrt{\beta}}\right] - 1875\beta^{5/2} \sinh\left[\frac{\bar{y} + 2\bar{y}_{\bar{\delta}}(\bar{x})}{\sqrt{\beta}}\right]\Bigg)\bar{y}_{\bar{\delta}}(\bar{x})
$$

$$
- 2\cosh\left[\frac{\bar{y}_{\bar{\delta}}(\bar{x})}{\sqrt{\beta}}\right] \Bigg(2310\bar{y}\beta^2(2\bar{y}^2 + 69\beta)\cosh\left[\frac{\bar{y}}{\sqrt{\beta}}\right] + 105\bar{y}\beta^2(22\bar{y}^2 + 867\beta)
$$

$$
\times \cosh\left[\frac{\bar{y} - 2\bar{y}_{\bar{\delta}}(\bar{x})}{\sqrt{\beta}}\right] + 6\bar{y}^7 \cosh\left[\frac{\bar{y}_{\bar{\delta}}(\bar{x})}{\sqrt{\beta}}\right] + 378\bar{y}^5\beta \cosh\left[\frac{\bar{y}_{\bar{\delta}}(\bar{x})}{\sqrt{\beta}}\right]
$$

$$
\begin{aligned}
&+ 191520\bar{y}\beta^3 \cosh\left[\frac{\bar{y}_{\bar{\delta}}(\bar{x})}{\sqrt{\beta}}\right] + 2\bar{y}^7 \cosh\left[\frac{3\bar{y}_{\bar{\delta}}(\bar{x})}{\sqrt{\beta}}\right] + 126\bar{y}^5\beta \cosh\left[\frac{3\bar{y}_{\bar{\delta}}(\bar{x})}{\sqrt{\beta}}\right] \\
&+ 70560\bar{y}\beta^3 \cosh\left[\frac{3\bar{y}_{\bar{\delta}}(\bar{x})}{\sqrt{\beta}}\right] + 2310\bar{y}^3\beta^2 \cosh\left[\frac{\bar{y}+2\bar{y}_{\bar{\delta}}(\bar{x})}{\sqrt{\beta}}\right] \\
&+ 91035\bar{y}\beta^3 \cosh\left[\frac{\bar{y}+2\bar{y}_{\bar{\delta}}(\bar{x})}{\sqrt{\beta}}\right] \\
&- 210\bar{y}^4\beta^{3/2} \sinh\left[\frac{\bar{y}}{\sqrt{\beta}}\right] - 38430\bar{y}^2\beta^{5/2} \sinh\left[\frac{\bar{y}}{\sqrt{\beta}}\right] - 282240\beta^{7/2} \sinh\left[\frac{\bar{y}}{\sqrt{\beta}}\right] \\
&- 105\bar{y}^4\beta^{3/2} \sinh\left[\frac{\bar{y}-2\bar{y}_{\bar{\delta}}(\bar{x})}{\sqrt{\beta}}\right] - 20475\bar{y}^2\beta^{5/2} \sinh\left[\frac{\bar{y}-2\bar{y}_{\bar{\delta}}(\bar{x})}{\sqrt{\beta}}\right] \\
&- 160650\beta^{7/2} \sinh\left[\frac{\bar{y}-2\bar{y}_{\bar{\delta}}(\bar{x})}{\sqrt{\beta}}\right] - 105\bar{y}^4\beta^{3/2} \sinh\left[\frac{\bar{y}+2\bar{y}_{\bar{\delta}}(\bar{x})}{\sqrt{\beta}}\right] \\
&- 20475\bar{y}^2\beta^{5/2} \sinh\left[\frac{\bar{y}+2\bar{y}_{\bar{\delta}}(\bar{x})}{\sqrt{\beta}}\right] - 160650\beta^{7/2} \sinh\left[\frac{\bar{y}+2\bar{y}_{\bar{\delta}}(\bar{x})}{\sqrt{\beta}}\right]\Bigg)\bar{y}_{\bar{\delta}}(\bar{x})^2 \\
&+ 70\beta^{3/2} \sinh\left[\frac{\bar{y}_{\bar{\delta}}(\bar{x})}{\sqrt{\beta}}\right]\Bigg(-4\bar{y}(2\bar{y}^2+165\beta)\cosh\left[\frac{\bar{y}}{\sqrt{\beta}}\right] - 2(2\bar{y}^3+165\bar{y}\beta) \\
&\times \cosh\left[\frac{\bar{y}-2\bar{y}_{\bar{\delta}}(\bar{x})}{\sqrt{\beta}}\right] \\
&+ 2760\bar{y}\beta \cosh\left[\frac{\bar{y}_{\bar{\delta}}(\bar{x})}{\sqrt{\beta}}\right] + 984\bar{y}\beta \cosh\left[\frac{3\bar{y}_{\bar{\delta}}(\bar{x})}{\sqrt{\beta}}\right] - 4\bar{y}^3 \cosh\left[\frac{\bar{y}+2\bar{y}_{\bar{\delta}}(\bar{x})}{\sqrt{\beta}}\right] \\
&- 330\bar{y}\beta \cosh\left[\frac{\bar{y}+2\bar{y}_{\bar{\delta}}(\bar{x})}{\sqrt{\beta}}\right] + 108\bar{y}^2\sqrt{\beta} \sinh\left[\frac{\bar{y}}{\sqrt{\beta}}\right] + 1506\beta^{3/2} \sinh\left[\frac{\bar{y}}{\sqrt{\beta}}\right] \\
&+ 54\bar{y}^2\sqrt{\beta} \sinh\left[\frac{\bar{y}-2\bar{y}_{\bar{\delta}}(\bar{x})}{\sqrt{\beta}}\right] + 825\beta^{3/2} \sinh\left[\frac{\bar{y}-2\bar{y}_{\bar{\delta}}(\bar{x})}{\sqrt{\beta}}\right] \\
&+ 54\bar{y}^2\sqrt{\beta} \sinh\left[\frac{\bar{y}+2\bar{y}_{\bar{\delta}}(\bar{x})}{\sqrt{\beta}}\right] \\
&+ 825\beta^{3/2} \sinh\left[\frac{\bar{y}+2\bar{y}_{\bar{\delta}}(\bar{x})}{\sqrt{\beta}}\right]\Bigg)\bar{y}_{\bar{\delta}}(\bar{x})^3 - 28\cosh\left[\frac{\bar{y}_{\bar{\delta}}(\bar{x})}{\sqrt{\beta}}\right]\Bigg(-450\bar{y}\beta^2 \cosh\left[\frac{\bar{y}}{\sqrt{\beta}}\right] \\
&- 225\bar{y}\beta^2 \cosh\left[\frac{\bar{y}-2\bar{y}_{\bar{\delta}}(\bar{x})}{\sqrt{\beta}}\right] - 3\bar{y}^5 \cosh\left[\frac{\bar{y}_{\bar{\delta}}(\bar{x})}{\sqrt{\beta}}\right] + 3060\bar{y}\beta^2 \cosh\left[\frac{\bar{y}_{\bar{\delta}}(\bar{x})}{\sqrt{\beta}}\right] \\
&- \bar{y}^5 \cosh\left[\frac{3\bar{y}_{\bar{\delta}}(\bar{x})}{\sqrt{\beta}}\right] \\
&+ 540\bar{y}\beta^2 \cosh\left[\frac{3\bar{y}_{\bar{\delta}}(\bar{x})}{\sqrt{\beta}}\right] - 225\bar{y}\beta^2 \cosh\left[\frac{\bar{y}+2\bar{y}_{\bar{\delta}}(\bar{x})}{\sqrt{\beta}}\right] + 30\bar{y}^2\beta^{3/2} \sinh\left[\frac{\bar{y}}{\sqrt{\beta}}\right] \\
&+ 690\beta^{5/2} \sinh\left[\frac{\bar{y}}{\sqrt{\beta}}\right] + 15\bar{y}^2\beta^{3/2} \sinh\left[\frac{\bar{y}-2\bar{y}_{\bar{\delta}}(\bar{x})}{\sqrt{\beta}}\right] + 150\beta^{5/2} \sinh\left[\frac{\bar{y}-2\bar{y}_{\bar{\delta}}(\bar{x})}{\sqrt{\beta}}\right] \\
&+ 15\bar{y}^2\beta^{3/2} \sinh\left[\frac{\bar{y}+2\bar{y}_{\bar{\delta}}(\bar{x})}{\sqrt{\beta}}\right] + 150\beta^{5/2} \sinh\left[\frac{\bar{y}+2\bar{y}_{\bar{\delta}}(\bar{x})}{\sqrt{\beta}}\right]\Bigg)\bar{y}_{\bar{\delta}}(\bar{x})^4 \\
&- 1680\beta^{3/2} \cosh\left[\frac{\bar{y}_{\bar{\delta}}(\bar{x})}{\sqrt{\beta}}\right]^2\Bigg(-2\bar{y}\cosh\left[\frac{\bar{y}}{\sqrt{\beta}}\right] + \bar{y}\cosh\left[\frac{\bar{y}_{\bar{\delta}}(\bar{x})}{\sqrt{\beta}}\right] + 13\sqrt{\beta}\sinh\left[\frac{\bar{y}}{\sqrt{\beta}}\right]\Bigg)
\end{aligned}
$$

$$\times \sinh\left[\frac{\bar{y}_{\bar{\delta}}(\bar{x})}{\sqrt{\beta}}\right]\bar{y}_{\bar{\delta}}(\bar{x})^5 - 14\beta\cosh\left[\frac{\bar{y}_{\bar{\delta}}(\bar{x})}{\sqrt{\beta}}\right]\left(-452\bar{y}\cosh\left[\frac{\bar{y}_{\bar{\delta}}(\bar{x})}{\sqrt{\beta}}\right]\right.$$
$$\left.- 148\bar{y}\cosh\left[\frac{3\bar{y}_{\bar{\delta}}(\bar{x})}{\sqrt{\beta}}\right]\right.$$
$$\left.+ 10\sqrt{\beta}\left(1 + 17\cosh\left[\frac{2\bar{y}_{\bar{\delta}}(\bar{x})}{\sqrt{\beta}}\right]\right)\sinh\left[\frac{\bar{y}}{\sqrt{\beta}}\right]\right)\bar{y}_{\bar{\delta}}(\bar{x})^6 - 448\bar{y}\cosh\left[\frac{\bar{y}_{\bar{\delta}}(\bar{x})}{\sqrt{\beta}}\right]^4\bar{y}_{\bar{\delta}}(\bar{x})^8)$$
$$+ \left(\left(-\bar{y}(\bar{y}^2 + 6\beta)\cosh\left[\frac{\bar{y}_{\bar{\delta}}(\bar{x})}{\sqrt{\beta}}\right] + 6\beta^{3/2}\sinh\left[\frac{\bar{y}}{\sqrt{\beta}}\right] + 3\bar{y}\cosh\left[\frac{\bar{y}_{\bar{\delta}}(\bar{x})}{\sqrt{\beta}}\right]\bar{y}_{\bar{\delta}}(\bar{x})^2\right)\right.$$
$$\times\left(929880\beta^{9/2}\cosh\left[\frac{\bar{y}_{\bar{\delta}}(\bar{x})}{\sqrt{\beta}}\right]\sinh\left[\frac{\bar{y}_{\bar{\delta}}(\bar{x})}{\sqrt{\beta}}\right]^3 - 2520\beta^4\left(137 + 122\cosh\left[\frac{2\bar{y}_{\bar{\delta}}(\bar{x})}{\sqrt{\beta}}\right]\right)\right.$$
$$\left.\times\sinh\left[\frac{\bar{y}_{\bar{\delta}}(\bar{x})}{\sqrt{\beta}}\right]^2\bar{y}_{\bar{\delta}}(\bar{x}) - 5985\beta^{7/2}\left(74\sinh\left[\frac{2\bar{y}_{\bar{\delta}}(\bar{x})}{\sqrt{\beta}}\right] + 25\sinh\left[\frac{4\bar{y}_{\bar{\delta}}(\bar{x})}{\sqrt{\beta}}\right]\right)\bar{y}_{\bar{\delta}}(\bar{x})^2\right.$$
$$\left.+ 420\beta^3\left(1103 + 1449\cosh\left[\frac{2\bar{y}_{\bar{\delta}}(\bar{x})}{\sqrt{\beta}}\right] + 322\cosh\left[\frac{4\bar{y}_{\bar{\delta}}(\bar{x})}{\sqrt{\beta}}\right]\right)\bar{y}_{\bar{\delta}}(\bar{x})^3\right.$$
$$\left.- 420\beta^{5/2}\left(164\sinh\left[\frac{2\bar{y}_{\bar{\delta}}(\bar{x})}{\sqrt{\beta}}\right] + 99\sinh\left[\frac{4\bar{y}_{\bar{\delta}}(\bar{x})}{\sqrt{\beta}}\right]\right)\bar{y}_{\bar{\delta}}(\bar{x})^4\right.$$
$$\left.+ 336\beta^2\cosh\left[\frac{\bar{y}_{\bar{\delta}}(\bar{x})}{\sqrt{\beta}}\right]^2\left(191 + 89\cosh\left[\frac{2\bar{y}_{\bar{\delta}}(\bar{x})}{\sqrt{\beta}}\right]\right)\bar{y}_{\bar{\delta}}(\bar{x})^5 + 28\beta^{3/2}\left(2\sinh\left[\frac{2\bar{y}_{\bar{\delta}}(\bar{x})}{\sqrt{\beta}}\right]\right.\right.$$
$$\left.\left.+ 21\sinh\left[\frac{4\bar{y}_{\bar{\delta}}(\bar{x})}{\sqrt{\beta}}\right]\right)\bar{y}_{\bar{\delta}}(\bar{x})^6 - 96\beta\cosh\left[\frac{\bar{y}_{\bar{\delta}}(\bar{x})}{\sqrt{\beta}}\right]^2\left(39 + 38\cosh\left[\frac{2\bar{y}_{\bar{\delta}}(\bar{x})}{\sqrt{\beta}}\right]\right)\bar{y}_{\bar{\delta}}(\bar{x})^7\right.$$
$$\left.+ 352\cosh\left[\frac{\bar{y}_{\bar{\delta}}(\bar{x})}{\sqrt{\beta}}\right]^4\bar{y}_{\bar{\delta}}(\bar{x})^9\right)\Big)\Big/\left(3\beta^{3/2}\sinh\left[\frac{\bar{y}_{\bar{\delta}}(\bar{x})}{\sqrt{\beta}}\right] - 3\beta\cosh\left[\frac{\bar{y}_{\bar{\delta}}(\bar{x})}{\sqrt{\beta}}\right]\bar{y}_{\bar{\delta}}(\bar{x})\right.$$
$$\left.+ \cosh\left[\frac{\bar{y}_{\bar{\delta}}(\bar{x})}{\sqrt{\beta}}\right]\bar{y}_{\bar{\delta}}(\bar{x})^3\right)\bar{y}'_{\bar{\delta}}[x]\Big)\Big/\left(26880\left(3\beta^{3/2}\sinh\left[\frac{\bar{y}_{\bar{\delta}}(\bar{x})}{\sqrt{\beta}}\right]\right.\right.$$
$$\left.\left.- 3\beta\cosh\left[\frac{\bar{y}_{\bar{\delta}}(\bar{x})}{\sqrt{\beta}}\right]\bar{y}_{\bar{\delta}}(\bar{x}) + \cosh\left[\frac{\bar{y}_{\bar{\delta}}(\bar{x})}{\sqrt{\beta}}\right]\bar{y}_{\bar{\delta}}(\bar{x})^3\right)^3\right).$$

References

[1] M. Ahrens, D. D. Joseph, and J. Y. Yoo, *Hyperbolicity and change of type in the flow of viscoelastic fluids through pipes*, Journal of Non-Newtonian Fluid Mechanics, 24 (1987), pp. 67–83.

[2] H. Bellout and F. Bloom, *Steady plane poiseuille flows of incompressible multipolar fluids*, International Journal of Non-Linear Mechanics, 28 (1993), pp. 503–518. MR1241108

[3] H. Bellout and F. Bloom, *On the higher-order boundary conditions for incompressible nonlinear bipolar fluid flow*, Quarterly of Applied Mathematics, LXXI (2013), pp. 773–785. MR3136995

[4] H. Bellout and F. Bloom, *Incompressible Bipolar and non-Newtonian Viscous Fluid Flow*, Advances in Mathematical Fluid Mechanics, Birkhäuser, 2014. MR3155182

[5] H. Bellout, F. Bloom, and J. Nečas, *Phenomenological behavior of multipolar viscous fluids*, Quarterly of Applied Mathematics, 50 (1992), pp. 559–583. MR1178435

[6] J. C. F. Chow and K. Soda, *Laminar flow in tubes with constriction*, Physics of Fluids, 15 (1972), pp. 1700–1706.

[7] J. Deiber, M. Peirotti, R. Bortolozzi, and R. Durelli, *Flow of Newtonian fluids through sinusoidally constricted tubes. Numerical and experimental results*, Chemical Engineering Communications, 117 (1992), pp. 241–262.

[8] J. H. Forrester and D. F. Young, *Flow through a converging-diverging tube and its implications in occlusive vascular disease — I: Theoretical development*, Journal of Biomechanics, 3 (1970), pp. 297–305.

[9] J. H. Forrester and D. F. Young, *Flow through a converging-diverging tube and its implications in occlusive vascular disease — II: Theoretical and experimental results and their implications*, Journal of Biomechanics, 3 (1970), pp. 311–316.

[10] M. Hemmat and A. Borhan, *Creeping flow through sinusoidally constricted capillaries*, Physics of Fluids, 7 (1995).

[11] A. Hundertmark-Zaušková and M. Lukáčová-Medvid'ová, *Numerical study of shear-dependent non-Newtonian fluids in compliant vessels*, Comput. Math. Appl., 60 (2010), pp. 572–590. MR2665658

[12] S. Kasivisvanathan, P. Kaloni, and K. Rajagopal, *Flow of a non-newtonian fluid through axisymmetric pipes of varying cross-sections*, International Journal of Non-Linear Mechanics, 26 (1991), pp. 777–792.

[13] P. K. Kitanidis and B. B. Dykaar, *Stokes flow in a slowly varying two-dimensional periodic pore*, Transport in Porous Media, 26 (1997), pp. 89–98.

[14] L. G. Leal, *Advanced Transport Phenomena: Fluid Mechanics and Convective Transport Processes*, Cambridge Series in Chemical Engineering, Cambridge University Press, Oct. 2010. MR2543501

[15] M. Lukáčová-Medvid'ová and A. Zaušková, *On the existence and uniqueness of non-Newtonian shear-dependent flow in compliant vessels*, SIAM Journal on Mathematical Analysis (2010).

[16] A. Montz, *Some Bipolar Viscous Fluid Flow Problems in Rigid and Compliant Domains*, PhD thesis, Northern Illinois University, May 2014. MR3251261

[17] A. Montz, H. Bellout, and F. Bloom, *Existence and uniqueness of steady flows of nonlinear bipolar viscous fluids in a cylinder*, Discrete and Continuous Dynamical Systems - Series B, 20 (2015), pp. 2107–2128. MR3423214

[18] J. Nečas and M. Šilhavý, *Multipolar viscous fluids*, Quarterly of Applied Mathematics, 49 (1991), pp. 247–265. MR1106391

[19] A. Quarteroni and L. Formaggia, *Mathematical Modelling and Numerical Simulation of the Cardiovascular System*, vol. 12 of Handbook of Numerical Analysis, Elsevier, 2004. MR2087609

[20] S. Sisavath, X. Jing, and R. W. Zimmerman, *Creeping flow through a pipe of varying radius*, Physics of Fluids, 13 (2001), pp. 2762–2772.

[21] S. Čanić, D. Lamponi, A. Mikelić, and J. Tambača, *Self-consistent effective equations modeling blood flow in medium-to-large compliant arteries*, SIAM J. Multiscale Analysis and Simulation, 3 (2005), pp. 559–596. MR2136164

[22] S. Čanić and A. Mikelić, *Effective equations modeling the flow of a viscous incompressible fluid through a long elastic tube arising in the study of blood flow through small arteries*, SIAM Journal on Applied Dynamical Systems, 2 (2003), pp. 431–463. MR2031281

[23] C. Wang, *Stokes flow through a tube with bumpy wall*, Physics of Fluids, 18 (2006).

[24] B. Wiwatanapataphee, *Modelling of non-Newtonian blood flow through stenosed arteries*, Dynamics of Continuous, Discrete and Impulsive Systems Series B: Applications and Algorithms, 15 (2008), pp. 619–634. MR2445555

[25] J. Y. Yoo and D. D. Joseph, *Hyperbolicity and change of type in the flow of viscoelastic fluids through channels*, Journal of Non-Newtonian Fluid Mechanics, 19 (1985), pp. 15–41.

Allen Montz
991 Oxford RD
Glen Ellyn, IL 60137
USA
E-mail address: allen.montz@gmail.com

Hamid Bellout
7240 Jematell Lane
Scottsdale, AZ 85266
USA
E-mail address: bellout@niu.edu

Frederick Bloom
2316 Crab Apple Terrace
Buffalo Grove, IL 60089
USA
E-mail address: fbloom4@gmail.com

Received November 26, 2022